Proc. R. Soc. Lond. B **229**, 111–150 (1986)
Printed in Great Britain

On the spatial spread of rabies among foxes

BY J. D. MURRAY[1], F.R.S., E. A. STANLEY[2] AND D. L. BROWN[3]

[1] *Centre for Mathematical Biology, Mathematical Institute, Oxford University, 24–29 St Giles, Oxford OX1 3LB, U.K.*

[2] *Center for Nonlinear Studies and Theoretical Division, Los Alamos National Laboratory, Los Alamos, New Mexico* 87544, *U.S.A.*

[3] *Center for Nonlinear Studies and Computing Division, Los Alamos National Laboratory, Los Alamos, New Mexico* 87544, *U.S.A.*

(*Received* 11 *April* 1986)

We present a simple model for the spatial spread of rabies among foxes and use it to quantify its progress in England if rabies were introduced. The model is based on the known ecology of fox behaviour and on the assumption that the main vector for the spread of the disease is the rabid fox. Known data and facts are used to determine real parameter values involved in the model. We calculate the speed of propagation of the epizootic front, the threshold for the existence of an epidemic, the period and distance apart of the subsequent cyclical epidemics which follow the main front, and finally we quantify a means for control of the spatial spread of the disease.

By way of illustration we use the model to determine the progress of rabies up through the southern part of England if it were introduced near Southampton. Estimates for the current fox density in England were used in the simulations. These suggest that the disease would reach Manchester within about 3.5 years, moving at speeds as high as 100 km per year in the central region. The model further indicates that although it might seem that the disease had disappeared after the wave had passed it would reappear in the south of England after just over 6 years and at periodic times after that.

We consider the possibility of stopping the spread of the disease by creating a rabies 'break' ahead of the front through vaccination to reduce the population to a level below the threshold for an epidemic to exist. Based on parameter values relevant to England, we estimate its minimum width to be about 15 km. The model suggests that vaccination has considerable advantages over severe culling.

1. INTRODUCTION

During the past few hundred years, Europe has been repeatedly subjected to rabies epidemics (Baer 1975). No one seems to know why rabies died out some 50 to 100 years before its current reappearance. The present epidemic is believed to have started in 1939 in Poland and it has moved steadily westward at a rate of 30–60 km per year, being slowed temporarily by such barriers as rivers, high mountains and autobahns. The red fox is the main carrier, and victim, of rabies in the current

epidemic, although most mammals are thought to be susceptible to the disease. An epidemic, which is mainly being propagated by racoons, is also moving rapidly up the east coast of America. Rabies, a viral infection of the central nervous system, is transmitted by direct contact. The dog is the principal transmitter of the disease to man. Although the incidence of rabies in man, at least in Europe and America, is now rare, with only very few deaths a year, it is a particularly horrifying disease for which there is no known case of a recovery once the disease has reached the clinical stage. Rabies is a disease that justifiably gives serious cause for concern.

The wavefront of the European epizootic is now very close to the north coast of France, in spite of various attempts to halt its progress by killing and vaccination of foxes (Lignieres 1982). In France, in 1980 alone, 314 cases of rabies in domestic animals were reported and 1280 cases in wild animals. Foxes account for about 70% of all recorded cases in Western Europe. It seems almost inevitable that in the future rabies will be introduced into Britain through the illegal importation of pets. The problem will be particularly serious in Britain because of the high urban density of foxes, dogs and cats (see figure 9, which is a map of England with the approximate fox density distribution). It is the comparatively high urban racoon density that is responsible for the current rapid spread of rabies up the east coast of America. It is important to understand how the rabies epizootic wavefront progresses into uninfected regions, what control methods might halt it and how the various parameters affect them. This paper is concerned with these specific spatial problems. The book edited by Bacon (1985) is specifically concerned with the population dynamics of rabies. As well as providing biological and ecological background and useful data on the disease, it presents some of the mathematical models currently being studied. Of particular relevance is the chapter by F. G. Ball.

In the region behind the front, rabies persists, with the number of cases reported in any small area fluctuating up and down every 2–7 years. Figure 1 shows typical fluctuations in the populations of susceptible, infected but not rabid, and rabid foxes after the passage of the epidemic front. It also gives approximate times and distances between the successive outbreaks. The figure was calculated from the model proposed and studied in this paper, by using parameters derived from published field studies relevant to the European continent. Figure 2 (in §3) shows the corresponding fox density fluctuations with parameters appropriate for England: it is qualitatively similar.

Because the fox is the main carrier of the rabies virus for the current epizootic, in the model we propose here we assume that the ecology of foxes determines the dynamics of the spread of rabies. Recently Källén *et al.* (1985) suggested that the spatial spread of the European epizootic is due primarily to the migration of rabid foxes. They studied a primitive model in which the fox population was divided into two groups, susceptible and rabid. Their model captures certain aspects of the spatial spread of the epizootic front, but it leaves out a basic feature of rabies, namely the rather lengthy incubation period of between 12 and 150 days from the time of an infected bite to the onset of the clinical infectious stage. Anderson *et al.* (1981) studied a model for the overall dynamics of the fox–rabies interaction, which takes this incubation period into account. They did not address the problem

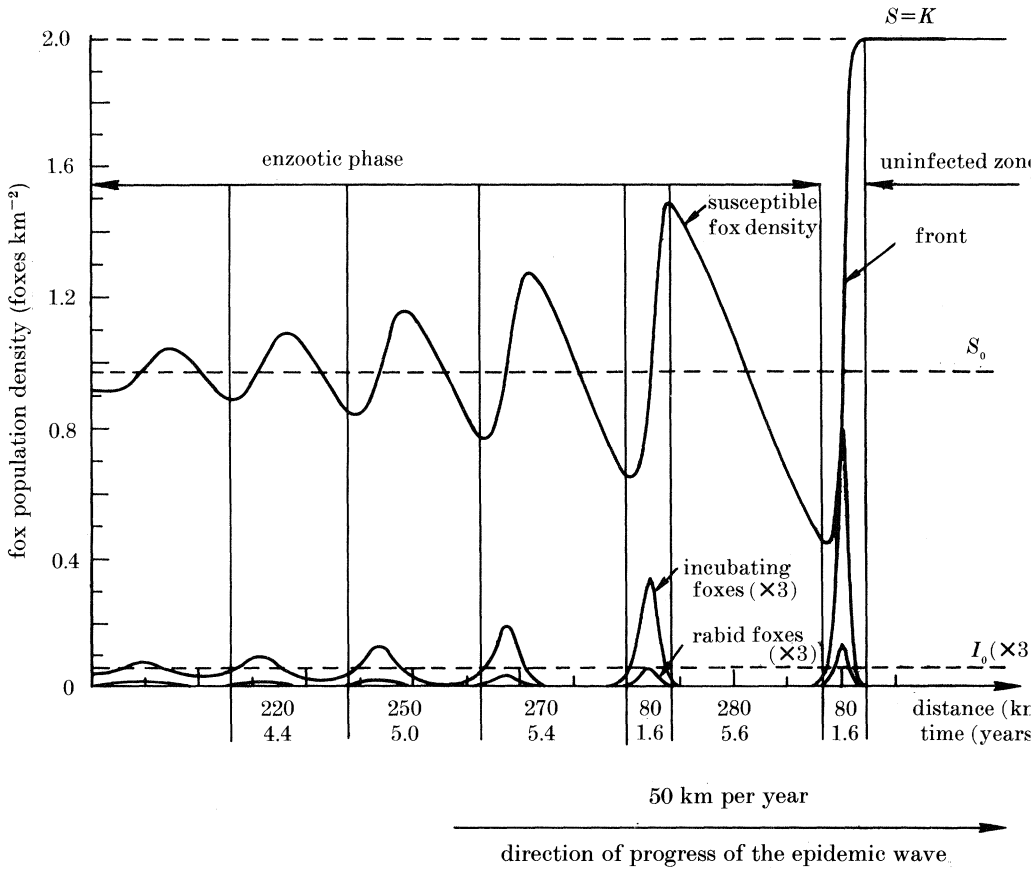

FIGURE. 1. Typical fluctuations in the fox populations due to the passage of a rabies epidemic wave as calculated from the model mechanism proposed in this paper (see §2, model system (1)). The fox density in the uninfected region ahead of the front of the epidemic is taken to be at a carrying capacity of 2 foxes km^{-2}, a typical value (averaged over the yearly cycle) for much of continental Europe. The infected population is not yet infectious: only rabid foxes are assumed to transmit the disease. The time and distance between the recurring outbreaks, and the wave speed, were obtained from the model by using estimates for the field parameters given in table 1 and a diffusion coefficient of 200 km^2 per year. (The details are given in §3.)

of spatial spread. In this paper we extend the Anderson *et al.* (1981) model to include the *spatial* spread of the disease. We assume that the main cause for the spread is the erratic movement of rabid foxes. Foxes do not colonize empty territory very quickly. Not only that, it appears that the incidence of rabies in young foxes, who disperse to seek their own territories, is not as high as in adult foxes (Artois & Aubert 1982; Macdonald 1980). It seems not unreasonable at this stage therefore to investigate this more realistic three-species model where the rabid foxes are the main cause of the spatial spread. Some of the rather scant data on the movement of rabid foxes in the wild are discussed in §4.

The motivation for continuing to study comparatively simple, deterministic models for such a complex problem is that the results highlight possible key

processes that may be occurring. They also raise questions that any model must address and that any control strategy must take into account. There is, as in any modelling, a trade-off between simplicity and the number of parameters that have to be estimated from field studies. Even with our simple model, which is derived in detail in §2, some of the parameters are difficult to estimate from the available data. In §4 we point out the importance of learning more about fox ecology and the impact of rabies on fox behaviour to improve upon the estimation of the more critical parameters. Tables 1 and 4 list the values we have been able to extract from the published literature. It should perhaps be mentioned again that we study here only the deterministic model. A fuller study should include stochastic effects, which are particularly important at low fox densities. Qualitative features of such models are to a certain extent independent of whether the model is deterministic or stochastic.

The existence of a threshold population for the existence of an epidemic in a spatially uniform population is well known. So if the susceptible fox density is below a certain critical value we do not expect the epizootic wave to be able to propagate, and rabies will die out. We determine a quantitative condition for this critical density in terms of the parameters of our model in §2.

Using the model and the parameter values we deduce, we consider the spatial spread of the rabies epizootic in §3 and determine the speed of propagation in terms of the parameters, such as the susceptible fox population, the spatial dispersal of rabid foxes, the incubation period and the life expectancy of a rabid fox. If the fox population density is estimated at different times as the rabies epizootic passes by, as in figure 1, the wave consists of two main parts. These are the epidemic wave front, through which the fox population rapidly decreases and in which the number of rabid foxes is greatest, and the tail where there are essentially periodic-like outbreaks of the disease. Formulae for the maximum number of rabid foxes in the first onslaught and the time between successive outbreaks of rabies in the endemic regions are obtained in terms of relevant *dimensionless groupings* of the parameters of the model. The introduction of non-dimensional parameters shows how different parameters can have equivalent effects.

A crucial assumption of the model mechanism is that the rabid foxes disperse in a random way, which we mimic as a simple diffusion process. The relevant parameter is then the diffusion coefficient on which the propagation speed critically depends. In §4 we discuss this in depth and investigate the sensitivity of the mechanism to parameter values. We show that some are considerably more important than others, which highlights the ecological aspects about which we would like to know more.

One means of stopping the epizootic front from moving into a rabies-free region is to reduce the *susceptible* fox population in a strip in front of the wave. This can be by vaccination, accomplished by dropping food containing vaccine as has been done in Switzerland, or by killing. There are powerful, and we believe overriding, advantages to the former because it reduces the colonization of empty territory with all the benefits that that implies, a major one being the reduction in the level of spatial movement by potentially infected foxes. In §5 we estimate the width in kilometres of a 'rabies break', that is a strip in which the susceptible population

is sufficiently reduced to stop the infection from passing into the rabies-free region on the other side of the 'break'. This involves a numerical simulation of the full system of equations that constitute the model.

The fox population in Britain is far from uniform, and the variable density affects the local wave-front speed of propagation substantially. To address the practical situation in England it is necessary to consider the two-dimensional problem of an epidemic wave moving through a variable fox density, which we do in §6. Using a two-dimensional numerical method on the full system of equations, we first investigate how the epizootic front travels past a patch of higher and of lower fox density. This gives some idea of how a higher fox density, for example, can have a focusing effect on the wavefront. We then took a rough map of estimated fox densities in England, namely figure 9, using the estimates given by Macdonald (1981), and ran our numerical code to see how quickly rabies might move up through various parts of England if rabies were introduced, by way of example, near Southampton. The epizootic wave-front position is given in figure 11 in terms of days from the initial infection. Such numerical simulations involve considerable computing time. The results presented here were carried out on a Cray-XMP48 computer at the Los Alamos National Laboratory in New Mexico.

2. Model mechanism for the spatial spread of rabies

Here we briefly recapitulate the Anderson *et al.* (1981) model and modify it to incorporate spatial dispersal of rabid foxes. It is this modified model that we use to study how an epizootic wave propagates outward from an initial source of rabies.

We divide the fox population into three groups: susceptible foxes, with a population density S; infected, but non-infectious, foxes, with a density I; and infectious, rabid foxes, R. This division is based on the relatively long incubation period of 12–153 days that the rabies virus undergoes in the infected animal, during which time the animal appears to behave normally and does not transmit the disease, and on the relatively short period (1–10 days) of clinical disease that follows (Sikes 1980; Winkler 1975; Toma & Andral 1977; Macdonald 1980).

The basic model assumptions are as follows.

(i) The dynamics of the fox population in the absence of rabies can be approximated by the simple logistic law

$$\mathrm{d}S/\mathrm{d}T = (a-b)\,(1-S/K)S,$$

where T is time, a is the birth rate, b is the intrinsic death rate, and K is the environmental carrying capacity; a, b and K are parameters that may vary according to the habitat, but are taken to be constant in time. The model thus neglects the seasonality of births and food supply, with S being the mean value of the population during the yearly cycle; a, b and K are also averaged out over the year.

(ii) Rabies is transmitted from rabid to susceptible fox: interspecies transmission is believed to be quite rare. Susceptible foxes become infected at an average rate per head βR, which is proportional to the number of rabid foxes present. The

transmission coefficient β, which measures the rate of contact between the two species, is a constant independent of environment.

(iii) Infected foxes become infectious at an average rate per head σ, where $1/\sigma$ is the average incubation time.

(iv) Rabies is invariably fatal, with rabid foxes dying at an average per capita rate α ($1/\alpha$ is the average duration of clinical disease).

(v) Rabid and infected foxes continue to put pressure on the environment, and to die of causes other than rabies, but they have a negligible number of healthy offspring.

We take into account the spatial spread of the rabies epizootic by including some basic facts about foxes relevant to dispersal effects of the rabid foxes (see, for example, Baer 1975; Macdonald 1980). We thus make the following further assumptions.

(vi) Foxes are territorial, and divide the countryside up into non-overlapping ranges.

(vii) Rabies is transmitted by direct contact between foxes, usually by biting.

(viii) Rabies acts on the central nervous system, inducing behavioural changes in the host. About half of infected foxes have so-called 'furious rabies', and exhibit the ferocious symptoms typically associated with the disease, while with the rest the virus affects the spinal cord, causing gradual paralysis. Foxes with furious rabies may become aggressive and confused, losing their sense of direction and territorial behaviour, and wandering randomly.

In our model we consider the major spatial dispersal to come from the random wandering of the rabid foxes, which we model by simple diffusion, as was also done by Källén *et al.* (1985). So we add a diffusion term to the equation for the rabid foxes.

All of these assumptions (i)–(viii) suggest the following model system, which governs the spatial and temporal evolution of the rabies epizootic:

$$\partial S/\partial T = (a-b)(1-N/K)S-\beta RS, \tag{1a}$$

$$\partial I/\partial T = \beta SR-\sigma I-[b+(a-b)N/K]I, \tag{1b}$$

$$\partial R/\partial T = \sigma I-\alpha R-[b+(a-b)N/K]R+D\partial^2 R/\partial X^2, \tag{1c}$$

where

$$N = S+I+R \tag{1d}$$

is the total fox population and D is the diffusion coefficient. Here for algebraic simplicity we have written the equations in one-dimensional form. We use the full two-dimensional form when we compute the spread of the disease in England, discussed in §6. This model neglects the spatial dispersal of rabies by young, itinerant foxes who may get bitten while in search of a territory and carry rabies with them before they become rabid. There is some justification for this since rabies is much less common in the young than in adults (Artois & Aubert 1982; Macdonald 1980).

The term $(a-b)N/K$ in each of the equations (1) represents depletion of the food supply by all foxes. Because rabid foxes presumably do not eat, it could be argued that N should be replaced by $S+I$. However, because rabid foxes represent a very small proportion of the total number of foxes, and $a-b$ is also small, it would make

little difference to the quantitative results whether or not this is done: the numerical simulations of the model confirm this.

In the spatially uniform situation, that is (1) with $D = 0$, Anderson *et al.* (1981) found that when rabies is introduced into a stable population of healthy foxes these equations predict three possible behaviours. If the carrying capacity of the system is below a critical value K_t, given by

$$K_t = (\sigma+a)(\alpha+a)/\beta\sigma, \tag{2}$$

then rabies eventually disappears, and the population returns to its initial value K. On the other hand, if K is larger than K_t, then the population oscillates about a steady state $S = S_0$, $R = R_0$, $I = I_0$, the steady-state solutions of (1), namely

$$S_0 = \beta^{-1}[\sigma\beta K - a(a-b)]^{-2}\{[(\alpha+b)\beta K + (a-b)(\alpha+a)][\sigma\beta K(\sigma+b) + \alpha(a-b)(\sigma+a)]\}, \tag{3a}$$

$$I_0 = [\sigma\beta K - a(a-b)]^{-1}[(\alpha+b)\beta K + (a-b)(\alpha+a)]R_0, \tag{3b}$$

$$R_0 = \{\beta[\sigma\beta K - a(a-b)]\}^{-1}(a-b)[\sigma\beta K - (\sigma+a)(\alpha+a)]. \tag{3c}$$

If K is not too much bigger than K_t, then the oscillations gradually damp out and the system approaches S_0, I_0, R_0, whereas if K is sufficiently large the system approaches a limit cycle periodic oscillation about that point. There are thus two bifurcation values for K, namely K_t and the critical K between a limit cycle oscillation and a stable steady state.

Epidemiological evidence supports the claim that rabies dies out if the carrying capacity is small enough; the critical value is somewhere between 0.2 and 1.0 foxes km^{-2} (WHO Report 1973; Macdonald 1980; Steck & Wandeler 1980; Anderson *et al.* 1981; Boegel *et al.* 1981); β, which is a measure of the contact rate between rabid and healthy foxes, cannot be estimated directly given the difficulty involved in observing these contacts. Inversion of (2) gives an indirect way to compute β, which is the method Anderson *et al.* (1981) used.

With $K > K_t$, the parameter choices, listed in table 1, give 3–5 year periods for the oscillations and 0–4% equilibrium persistence of rabies, defined by

$$p = (R_0+I_0)/(S_0+I_0+R_0), \tag{4}$$

which is in agreement with the available epidemiological evidence (Toma & Andral 1977; Macdonald 1980; Steck & Wandeler 1980; Jackson & Schneider 1984).

TABLE 1. PARAMETER VALUES USED BY ANDERSON *ET AL.* (1981)

parameter	symbol	value
average birth rate	a	1 per year
average intrinsic death rate	b	0.5 per year
average duration of clinical disease	$1/\alpha$	5 days
average incubation time	$1/\sigma$	28 days
carrying capacity	K_t	1 fox km^{-2}
disease transmission coefficient	β	80 km^2 per year
carrying capacity	K	0.25 to 4.0 foxes km^{-2}

3. Spatial spread of the rabies epizootic and its speed of propagation

To get an understanding of the behaviour predicted by the model system (1), we first consider the case of a uniform environment in which all parameters are constants. We are interested in the dynamics of the fox population when a few rabid foxes are introduced into an initially stable rabies-free population.

It is, as always, instructive to introduce non-dimensional quantities, here by

$$\left.\begin{aligned} &s = S/K, \quad q = I/K, \quad r = R/K, \quad n = N/K, \\ &\epsilon = (a-b)/\beta K, \quad \delta = b/\beta K, \quad \mu = \sigma/\beta K, \quad d = (\alpha+b)/\beta K, \\ &x = (\beta K/D)^{\frac{1}{2}} X, \quad t = \beta K T. \end{aligned}\right\} \tag{5}$$

This allows us to determine the effective parameter groupings in the system, and to obtain a qualitative understanding of the system in terms of them.

With (5) the model equations (1) become

$$\partial s/\partial t = \epsilon(1-n)\, s - rs, \tag{6a}$$

$$\partial q/\partial t = rs - (\mu+\delta+\epsilon n)\, q, \tag{6b}$$

$$\partial r/\partial t = \mu q - (d+\epsilon n)\, r + \partial^2 r/\partial x^2, \tag{6c}$$

$$n = s+q+r, \tag{6d}$$

which have a positive uniform steady-state solution (s_0, q_0, r_0) given by (3) on dividing by K.

The behaviour of this system now depends only on the four dimensionless parameters, ϵ, δ, μ and d: the original system involves seven parameters. The actual values of these dimensionless parameters are obtained from the physical parameters, a, b, α, σ, K and β. At a carrying capacity of two foxes km^{-2} the values in table 1 give $\epsilon = \delta = 0.003$, $\mu = 0.08$, and $d = 0.46$. A major benefit of non-dimensionalization is that the parameters display equivalent effects of variations in actual field parameters. We see from these values that ϵ and δ are relatively small numbers compared with any of $1, \mu, d$ and $1-d$, a fact that can be used to simplify the analysis of system (6) and allow us to derive useful analytical results, which we discuss below (and which are derived in the Appendixes). Physically what this means is that the infection rate is very much larger than the birth and death rates from causes other than rabies during the epidemic.

Solving system (6) numerically, starting with $s = 1$ (that is $S = K$) everywhere and with a small concentration of rabid foxes at the origin, gives two different results, depending on the size of K. If $K > K_t$, the critical carrying capacity for an epidemic, or, equivalently in non-dimensional form,

$$d < [1+(\delta+\epsilon)/\mu]^{-1} - \epsilon, \tag{7}$$

an epidemic wave forms and travels outward from the initial concentration of rabid foxes with near-constant velocity. If, however, inequality (7) is violated, then rabies dies out, and the fox population returns to the carrying capacity of the environment, just as it does for system (1) with $D = 0$. An example of the travelling wave that forms when (7) is satisfied is shown in figure 1 above. This wave consists of the rabies front, in which the largest number of foxes die from the disease,

followed by an oscillatory tail, in which each successive outburst of rabies is smaller than the preceding one. The oscillations gradually approach constant, non-zero values with the rabid and infected fox population zero. Figure 2 illustrates the fluctuations in fox density for a travelling wave with parameters appropriate for England.

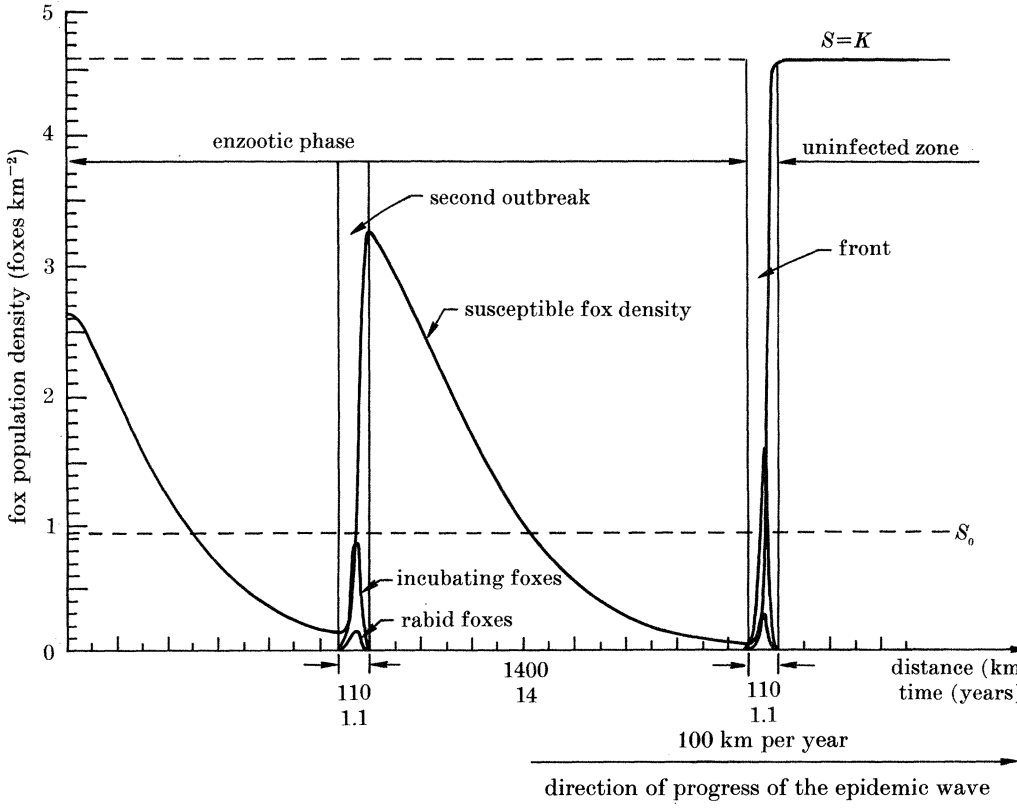

FIGURE 2. Fox populations during the passage of the rabies epidemic wave as predicted by our model (system (6)) when the fox density in front of the epidemic is at the carrying capacity of 4.6 foxes km^{-2}, which is common in parts of England. D was assumed to be 200 km^2 per year, and the other parameters were taken from table 1.

If we look for an analytical solution to system (6) which travels at a constant non-dimensionalized velocity v (see Appendix 1 for details), it can be shown that such a solution cannot exist unless relation (7) holds. Assuming that (7) is satisfied, and, based on the parameter values in table 1, that

$$\epsilon \text{ and } \delta \ll 1,\ d,\ \mu \text{ and } 1-d, \tag{8}$$

we find that the shape of the wave is the same as that found numerically, namely a front followed by an oscillatory tail that moves into the rabies-free region. The minimum speed at which the wave can travel is given by $v = z^{\frac{1}{2}}$, where z is the unique positive root of the cubic.

$$g(z) = [4\mu+(d-\mu)^2]z^3+2[3\mu(1-d)(3d+\mu)+(d+\mu)^2(2d+\mu)z^2 + \mu^2[(d+\mu)^2-6(1-d)(3d+\mu)-27(1-d)^2]z-4\mu^4(1-d), \tag{9}$$

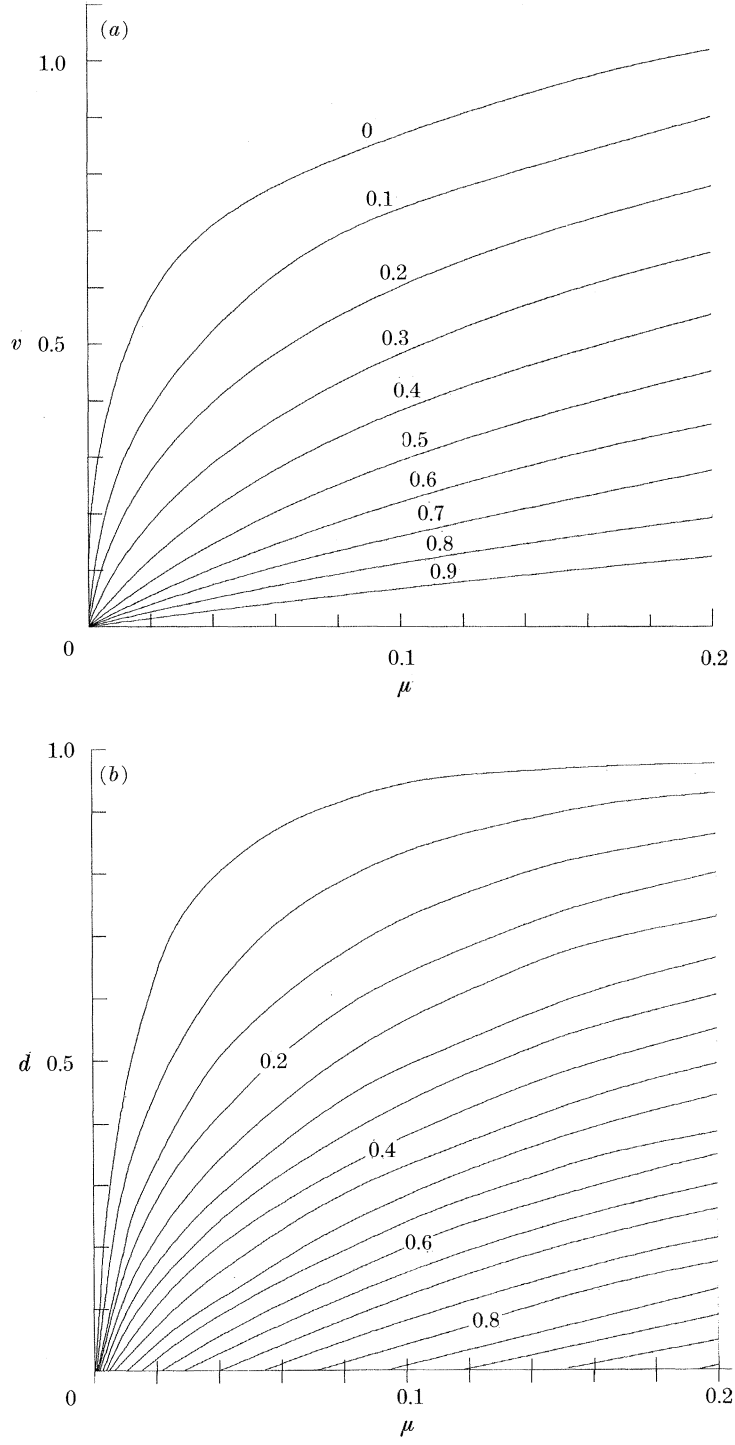

FIGURE 3. For description see opposite.

to first order in ϵ and δ. A contour plot for this root $v(=z^{\frac{1}{2}})$ is shown in figure 3 for $0 \leqslant d \leqslant 1$. The waves found numerically appear to travel at this minimum speed, $v = z^{\frac{1}{2}}$ or, in dimensional form $V = (D\beta Kz)^{\frac{1}{2}}$. For example, with the parameter values in table 1, a diffusion coefficient of 200 km^2 per year and a carrying capacity of 2 foxes km^{-2}, the speed of propagation V is 51 km per year.

The uniform state (s_0, q_0, r_0) about which the wave oscillates is simply the dimensionless form of the steady state of system (1) which was given by (3) in dimensional form. A linear analysis near the point s_0, q_0, r_0, shows that, for sufficiently large times, the wave tends to decaying oscillations of the form

$$s(x, t) = s_0 + A\cos[\omega(t+x/v)+\psi]\exp[-\lambda(t+x/v)], \tag{11a}$$

$$q(x, t) = q_0 + \mu^{-1}(s-s_0)', \tag{11b}$$

$$r(x, t) = r_0 + \mu(q-q_0)/d, \tag{11c}$$

to first order in ϵ and δ, where the prime denotes differentiation with respect to $t+x/v$, and the non-dimensional wave number ω is given by

$$\omega = \epsilon^{\frac{1}{2}}[\mu d(1-d)/(\mu+d)]^{\frac{1}{2}} + O(\epsilon^{\frac{3}{2}}), \tag{12}$$

with the decay rate λ by

$$\lambda = \epsilon d[2(\mu+d)^2]^{-1}[\mu(\mu/v^2-1)(1-d)+(\mu+d)^2]. \tag{13}$$

A and ψ are constants. Note that the oscillations in the susceptible population are 90° out of phase with both the infected and the rabid populations and that r and q are related by $r-r_0 \approx (q-q_0)\mu/\mathrm{d}$. (This symmetry is broken if the oscillations are calculated to the next order in ϵ and δ). This r–q relation correlates with the long-time behaviour in figures 1 and 2. Note also that to first order in ϵ and δ (see Appendix 1) the steady-state $r_0 = \mu q_0/d$ so that far enough behind the front of the wave r and q are proportional to each other. In the numerical simulations this proportionality always seems to hold when the physically reasonable parameters are used. In Appendix 1 we use a nonlinear scaling technique to show that this is in fact implied by the model equations. The mathematical analysis is based on the observation that μ is small compared with both d and the non-dimensional wavespeed, but large compared with ϵ and δ.

In Appendix 1 we derive an estimate for the maximum density of infected and of rabid foxes in the first outbreak, namely

$$r_{\max} \approx \mu[\ln d + (1-d)/d],$$

$$q_{\max} \approx d[\ln d + (1-d)/d],$$

FIGURE 3. The dimensionless velocity of propagation, v, of the epidemic front as a function of the dimensionless parameters μ and d. μ is related to the incubation time for the rabies virus, and d is related to the duration time of the symptomatic, infectious, stage: equations (5) give the expressions for these in terms of the field parameters of the model. The actual dimensional wave speed is given by $(\beta KD)^{\frac{1}{2}}v$. Note that $d = 0$ for $v \geqslant 1$ (see (5) for d in terms of the field parameters), which corresponds to a carrying capacity less than the critical value. (*a*) Velocity v as a function of μ, for μ varying from 0 to 0.2 (the range of physical interest when d is less than 1). Each curve is for a different value of the parameter d. (*b*) Contour lines of constant velocity v as a function of μ and d. Contour intervals are 0.05.

which in dimensional terms are

$$R_{\max} \approx (\sigma K_t/\alpha)\,[\ln(K_t/K) + K/K_t - 1],$$
$$Q_{\max} \approx K_t[\ln(K_t/K) + K/K_t - 1].$$

Thus both $R_{\max}$ and $Q_{\max}$ are zero for $K = K_t$ and increase as K increases above K_t.

Comparison of expression (13) for the decay rate with equation (9) shows that λ is always positive, and thus the limit cycle behaviour which system (1) exhibits for large K and $D = 0$ disappears when diffusion is taken into account: the oscillations always decay to the constant state s_0, q_0 and r_0.

Using the values in table 1, we can obtain estimates for the percentage reduction in population due to rabies (at equilibrium), $100\,(1-n_0)\,\% = 100\,[1-(s_0+q_0+r_0)]\,\%$, and the persistence of rabies,

$$p = (q_0+r_0)/n_0.$$

We can calculate the non-dimensional wavespeed v from the positive root of $g(z)$, and both the dimensional period and decay rate $\Lambda = \beta K\lambda$. The period is given by

$$\tau = 2\pi/(\beta K\omega)$$

or, writing it purely in terms of the original parameters,

$$\tau = 2\pi\{(\alpha+\sigma+b)\,[(a-b)\,(\alpha+b)\,\sigma\{1-(\alpha+b)/\beta K\}]^{-1}\}^{\frac{1}{2}}. \tag{14}$$

τ decreases with K. So, in general, the greater the fox density before the appearance of rabies, the less frequently rabies outbreaks will appear far behind the front, which agrees with some observations (Macdonald 1980). However, numerically we found that close to the front, where nonlinearities are important, the time between outbreaks may increase with K: see figures 1 and 2. The quantities n_0, p, v and λ all depend on K. To first order in ϵ and δ, n_0 is just K_t/K, so that another prediction of the model is that the fox density $n_0 K$ behind the rabies front oscillates about (and eventually decays to) a value close to the critical value. The percentage of rabid foxes at equilibrium, although never large, will be greater in the more hospitable environments, since the persistence is

$$p = (a-b)\,(1-K_t/K)\,[(\sigma+\alpha)/\sigma\alpha]. \tag{15}$$

Values for these five quantities are shown in table 2 for various values of the carrying capacity: K varies from 0.25 to 6 foxes km^{-2} in Europe (Lloyd *et al.* 1976; Toma & Andral 1977; Steck & Wandeler 1980). For example, at $K = 2$ foxes km^{-2}, which is typical of much of France and Germany, the estimates in table 1 give $n_0 = 0.47$, $p = 0.02$, $\tau = 3.7$ years, $\lambda = 0.11$ per year, $v = 0.3$.

Besides the carrying capacity, the growth rate, $a-b$, may also depend on the environment. Lloyd *et al.* (1976) found the birth rate all over Europe to be about the same (a between 1.0 and 1.1 per year), but because the intrinsic death rate depends on such local factors as hunting intensity and climate, the growth rate varies with environment. The speed of the rabies wave, as predicted by our model, is not affected (to first order) by this, nor is the number of foxes after oscillations

TABLE 2. DEPENDENCE OF PARAMETERS ON CARRYING CAPACITY, CALCULATED FROM THE VALUES IN TABLE 1

carrying capacity or K/K_t[(a)] K (foxes km^{-2})	time between successive peaks τ (years)	equilibrium fox density/K n_0	persistence of rabies p	decay rate Λ (year^{-1})	non-dimensional front velocity v
1.5	4.2	0.62	0.02	0.14	0.22
2.0	3.7	0.47	0.02	0.11	0.28
2.5	3.3	0.38	0.03	0.10	0.36
3.0	3.2	0.32	0.03	0.089	0.41

[(a)] The parameters β and K only appear as the product βK in the calculations for the values in tables 2–4. From (3), $\beta K = (K/K_t)(\sigma+a)(\alpha+a)/\sigma$, so that only a knowledge of the ratio of the actual carrying capacity to the critical value is necessary to obtain the results.

die out. However, when the growth rate is higher, and carrying capacities are similiar, the outbreaks of rabies behind the front will be more frequent, with their amplitude decaying more rapidly, and the percentage of rabid foxes at equilibrium will be greater. Values of b from 0.37 to 0.67 per year have been observed in Europe (Anderson *et al.* (1981). At a carrying capacity of 2 foxes km^{-2}, and with all values besides b taken from table 1, τ is 3.2 years for $b = 0.37$ per year and 4.5 years for $b = 0.67$ per year, p goes from 0.28 to 0.15 as b increases and Λ decreases from 0.15 to 0.08 per year.

To calculate either the speed V of the epizootic, or the wavelength $L = V\tau$ of the oscillations in the tail, we need an estimate for the diffusion coefficient. We discuss this problem, along with the sensitivity of our quantitative results to the physically measurable parameters, in the next section.

4. ESTIMATES FOR THE DIFFUSION COEFFICIENT: SENSITIVITY OF THE MODEL TO PARAMETER VALUES

To transform the velocity of the wavefront and the wavelengths of the oscillations in the tail into dimensional quantities, we need an estimate for the diffusion coefficient D, which is a measure of the rate at which a rabid fox covers ground in its wanderings. Little is known about the behaviour of rabid foxes in the wild, making it very difficult to estimate D.

Andral *et al.* (1982) have tracked three rabid adult foxes in the wild. They accomplished this by inoculating captured foxes with rabies virus, equipping them with signal-emitting collars, and releasing them at the point of capture. They traced the fox movements first during the incubation period, to determine their home ranges and normal behaviour, and then during the rabid period, to observe the changes induced by the disease. According to their observations, all three foxes became more agitated once the clinical phase of the disease commenced, and the pattern of daily activity changed. Drawings showing, for each fox, the incubation period range and the principal displacements during the rabid period indicate that all three left their home range at some point during the rabid phase, but none travelled very far away.

We can use the results of Andral *et al.* (1982) to estimate, in a crude manner, the diffusion coefficient from the formula

$$D \approx \frac{1}{N} \sum_{j=1}^{N} \frac{(\text{straight line distance from the start})^2}{4 \times (\text{time from the start})},$$

where the sum is over the number of all foxes involved. Use of the distance between the start of the rabid period and the point of death, along with the approximate length of the rabid period, gives an estimate of 50 km^2 per year for D. Since two of the three foxes happened to die much closer to their starting position than their mean distance away from it, this is most probably a lower bound on D. An extremely rough idea of an upper bound can be gained from the maximum distance that any one fox travelled away from its starting point. About halfway through the rabid phase, one fox got as far away from its starting point as 2.7 km, giving an estimate of 330 km^2 per year as an upper bound on D. There are other ways of estimating diffusion coefficients. For example, D can be estimated as the product of the average territory size A and the average rate k at which a rabid fox leaves home. For their two-species model, Källén *et al.* (1985) suppose that infected foxes leave home at the end of the incubation period of one month, i.e. upon becoming rabid. Taking an average territory size to be about 5 km^2, they obtained $D = 60$ km^2. To determine D for our three-species model, we need an estimate for the average rate at which foxes leave their territories *after* the onset of clinical disease. If N infected foxes are observed, and the jth one leaves its territory at time interval t_j after becoming rabid, then k can be estimated by

$$N^{-1} \sum_{j=1}^{N} t_j^{-1}.$$

Since roughly half of all infected foxes develop paralytic rabies (see assumption 8), and presumably never leave their home range, t_j, is infinite for about $\frac{1}{2}N$ foxes. For the furiously rabid foxes, if we suppose that half also never leave, and that the rest leave evenly spread out over the 6 days that the disease may take to run its course, then we can estimate

$$k \approx \frac{1}{N} \sum_{j=1}^{N/4} t_j^{-1} = \frac{1}{24} \sum_{j=1}^{6} \frac{1}{j \text{ days}} = 40 \text{ per year}.$$

Keeping the estimate of 5 km^2 for an average territory size (Toma & Andral 1977; Macdonald 1980), this gives $D = 190$ km^2 per year.

An alternative method is to estimate the mean free path and velocity of rabid foxes. The average total distance covered daily by the foxes observed by Andral *et al.* (1977) was 9 km during the rabid period. Suppose that this is not atypical, and that, for example, a rabid fox goes 100 m at a stretch before becoming distracted and setting off in another direction. Then $D = (\text{velocity}) \times (\text{pathlength})$ gives a diffusion coefficient of 330 km^2 per year, the same as the upper bound that we estimated previously. All of these methods for estimating D should, in principle, be consistent, if enough observations of rabid fox behaviour could be made. But there is simply not enough known about fox behaviour to get much better estimates.

Because the speed of the wave is proportional to $D^{\frac{1}{2}}$, changing D from 50 to 330 km^2 per year increases V by a factor of 2.6. If we look at table 2 we see that this means that, at $K = 2$ foxes km^{-2}, we can get a velocity of anywhere from 25 to 65 km per year depending entirely on the value we choose for D. Although our estimates for D are not good enough for us to give a firm quantitative prediction of the speed of the wave, we can arrive at a range of speeds that are reasonable when compared with the available data. By the same token, we cannot predict wavelengths in the tail of the wave with great accuracy but again the results we obtain compare reasonably with observation. This diffusion-coefficient inaccuracy does not, however, prevent us from looking at the manner in which V and L depend on the carrying capacity. This is done in table 3 by using the same parameter values as before.

TABLE 3. DEPENDENCE OF THE WAVE SPEED AND ASYMPTOTIC WAVE LENGTH (THAT IS THE DISTANCE BETWEEN RECURRING OUTBREAKS) ON THE CARRYING CAPACITY, CALCULATED WITH $D = 200$ KM^2 PER YEAR AND THE VALUES IN TABLE 1

K (foxes km^{-2}) or K/K_t: carrying capacity	V (km per year): velocity of the epidemic front	L (km): distance between successive outbreaks or peaks
1.5	35	150
2.0	50	210
2.5	70	220
3.0	80	250

The most difficult parameter to estimate, after D, is the disease transmission coefficient, β. Even less is known about contacts between rabid and healthy foxes than is known about the movements of rabid foxes, but β can be found from (2) and knowledge of the critical density. From (2), we see that β is proportional to $1/K_t$. The calculations in tables 2 and 3 do not depend independently on either K or β but only on their product, and thus on the ratio K/K_t (K alone is only important if we wish to calculate the actual density of foxes present at a given time from the dimensionless s, q, or r). Absolute values of fox population densities are, in practice, difficult to obtain; they are usually estimated from the numbers of foxes reported dead, shot or gassed, and some assumption on the percentage of the total population that this sample represents, or else by comparison of terrain with areas of known fox densities. K_t is particularly difficult to estimate, and values of anywhere from 0.2 to 1.2 foxes km^{-2} can be estimated from the values given in the literature (WHO Report 1973; Steck & Wandeler 1980; Macdonald *et al.* 1981; Gurtler & Zimen 1982). Since finding K/K_t only involves comparison of population sizes, this ratio might be easier to obtain than K and K_t separately.

A relevant question at this point is how sensitive the quantitative results in table 2 and 3 are to the uncertainties in the remaining parameters in our model. We have already discussed the dependence of these calculations on the growth rate $a-b$ and the carrying capacity in the last section. The uncertainties in the remaining three independent parameters, b, α and σ, do not appear to be as

important. b does not appear in the first-order results, since it is involved in δ, which is small and has no effect on the first-order analysis. The uncertainties in the other two values also do not have a major effect on the physically relevant parameters in tables 2 and 3. The average incubation time is generally considered to be somewhere between 25 and 30 days (Winkler 1977; Toma & Andral 1977; Macdonald 1980) which means that σ is probably in the interval of 11.4–14.6 per year, which is a relatively small interval of uncertainty. The range for α is, however, large: the average duration of clinical disease varies from 3 to 6 days, implying that α may be anywhere from 60.6 to 122 per year (Sikes 1970; Winkler 1985; Toma & Andral 1977). The effect of this range on the values in tables 2 and 3 is shown in table 4. Although the values for some quantities, such as β and v, change markedly when α varies over this interval, the physically relevant quantities do not greatly change.

ABLE 4. SENSITIVITY OF MODEL PREDICTIONS TO THE UNCERTAINTY IN α, THE RABID FC DEATH RATE, CALCULATED FROM ALL OTHER VALUES FROM TABLE 1, $K/K_t = 2$ AN $D = 200$ km^2 PER YEAR

average duration of clinical disease α^{-1} (days)	transmission coefficient β (km^2 per year)	ratio of equilibrium fox density to carrying capacity n_0	persistence of rabies p	time between successive outbreaks τ	decay rate λ (year^{-1})	velocity of the epidemic V (km per year)	distance between successive outbreaks L (km)
3	132	0.5	0.02	3.5	0.11	45	160
4	99	0.5	0.02	3.5	0.11	49	170
5	80	0.5	0.03	3.6	0.11	51	180
6	67	0.5	0.02	3.6	0.12	52	190

5. EPIZOOTIC WAVE PROPAGATION INTO A NON-EPIDEMIC REGION: CONTROL MEASURES

A possible protective barrier against the rabies epizootic can be achieved by reducing the susceptible fox population below the critical density in areas ahead of the advancing wave. This, for example, has been successful in Denmark, specifically Jutland. It has also been carried out in some regions of Italy and Switzerland, where it has been pursued with diligence, but it has had mixed results (Irsara *et al.* 1982; Macdonald 1980; Westergaard 1982). Such a barrier can be created by either killing or vaccination. Since killing releases territories there could be a more rapid colonization by young foxes, which could enhance the spread of the disease. Vaccination causes less disruption in the ecology, and is probably even more economic.

For a rabies 'break' to be effective we must have reasonable estimates of both the width and the allowable susceptible fox density within it. Here we use our model to obtain estimates for how wide the protective break region needs to be to keep rabies from reaching the areas beyond. In what follows, we use the term 'infected fox' to refer to all foxes with rabies, whether infectious or not.

If we observe the passage of the rabies epizootic wave at a fixed place we note that each outbreak of the disease is followed by a long quiescent period, during

which very few cases of rabies occur (see figures 1 and 2). The spatial and temporal dimensions, as indicated in figure 1, are such that the secondary epidemic wave is far enough behind for the first either to have moved past the break, or to have effectively died out by the time that the second one arrives. Each successive outbreak is weaker than the previous one. It therefore seems reasonable to assume that the same population reduction schemes that eradicate the first outbreak will also be effective in stopping all future outbreaks from passing through. We thus only need to consider how wide the break needs to be to stop the first outbreak. The width of the break is dependent on the size of the susceptible fox population density within it. Figure 6 below gives the width of the break plotted against the carrying capacity for various values of relevant parameters.

Because we model spatial dispersal by a deterministic diffusion mechanism it is strictly not possible for the density of infected foxes to vanish anywhere. This is an artefact that arises from treating the fox densities as continuous in space and time, rather than dealing with individual foxes, and from using classical diffusion to model the rabid fox dispersal. Thus we cannot simply have the epizootic wave move into a break of finite width and determine whether or not the density of infected foxes remains zero on the other side: it will always be positive, although exponentially small. From a strict mathematical point of view, no matter how wide the break is, eventually enough infected fox density will in time leak through for the epizootic to start off again on the other side. Thus we must think instead of determining when the probability is acceptably small that an infected fox will reach the far side of the break.

Since the intent of any population reduction scheme is to hold the density of foxes at a low value, we treat the break region as one with a carrying capacity below K_t, the critical threshold value for persistence of an epidemic, and we assume that the fox density has been reduced to this value well before the epizootic front arrives. To obtain estimates for the width of the break we investigate the behaviour of the model when the region of lowered susceptible fox density starts at $x = 0$ and extends to infinity. In figures 4 and 5 we show what happens when the epizootic wave, coming in from the left, impinges on the break region. Recall that the epizootic wave cannot propagate when the carrying capacity is below the critical value K_t, and also that the point of maximum infected fox density will be at $x = 0$. As the infection wave moves into the region $x > 0$ it spreads out, decays in amplitude and the total number of infected foxes decreases. Eventually there will be less than p infected foxes km^{-2} remaining, where p is some small number. Let $t_c(p)$ be the time at which this occurs. We now choose p sufficiently small that the probability of a rabid fox's encountering a healthy one after this critical time is negligible. Since the wave cannot propagate in the break region it simply decays, so for all time the density of infected foxes is greatest at the edge of the break and decays exponentially in x – exponentially as x^2 in fact. We choose the width of the break to be the point x_c, where the infected fox density is a given (small) fraction m of the value at the origin, that is

$$I(x_c, t_c) + R(x_c, t_c) = m[I(0, t_c) + R(0, t_c)]. \tag{16}$$

As far as we know, it has never proved possible to eliminate all foxes from a region. A 70% reduction in population is about the best that can be done

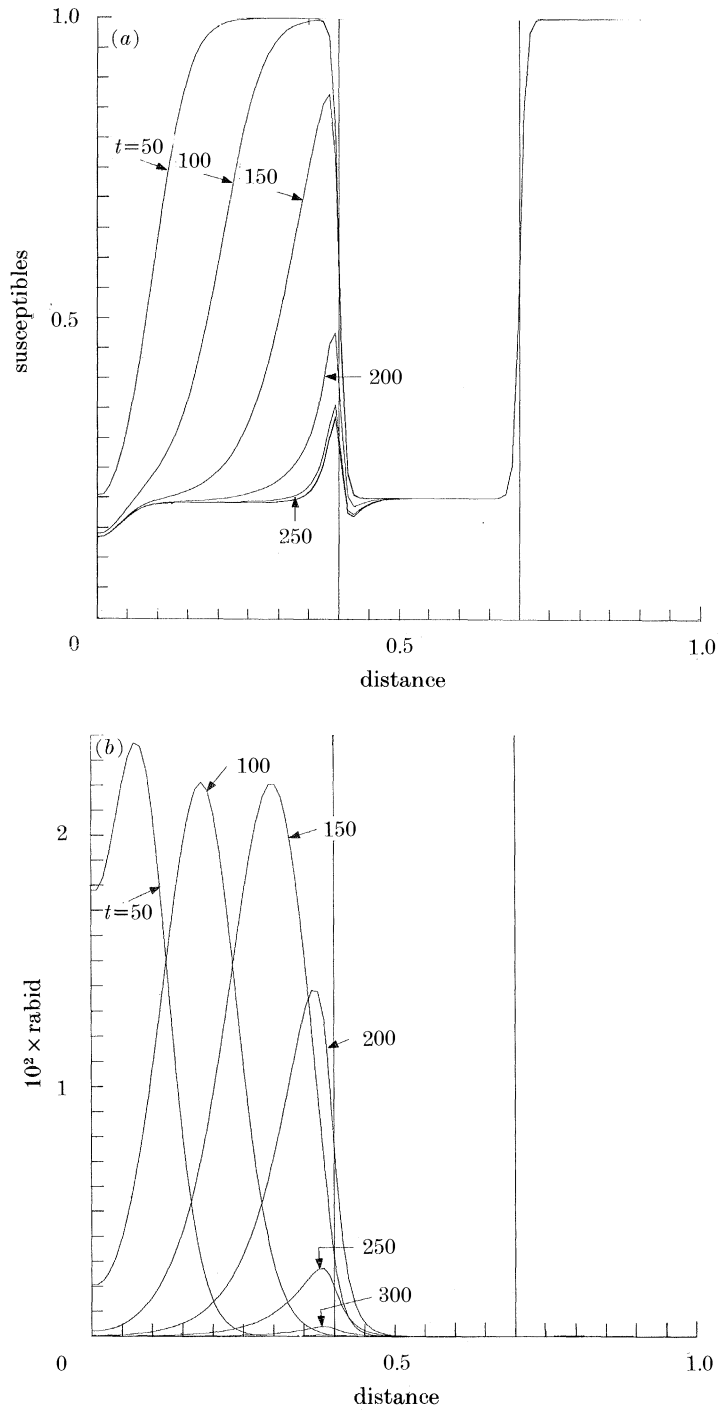

FIGURE 4. For description see opposite.

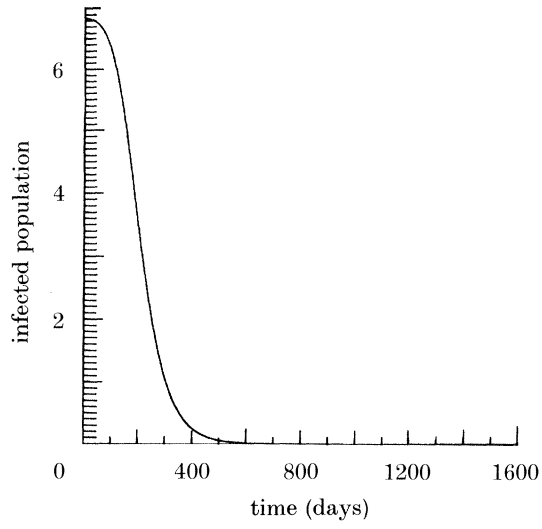

FIGURE 5. The decay of the rabid fox population in the first outbreak once the epidemic reaches the break region. This plot shows the total infected fox density per kilometre (the integral over x of $I+R$) as a function of time for the case shown in figure 4, starting when the epidemic front first reaches the break.

(Macdonald *et al.* 1981). The less effective the removal scheme, the wider the break has to be. Figure 6 shows this dependence in terms of the percentage population reduction in the break, for different choices of the average duration time of clinical disease, $1/\alpha$. In generating the curves in figure 6, βK outside the break was held at 160 per year, the number of infected foxes at the critical time was taken to be $p = \frac{1}{2}$ foxes km^{-2}, the ratio m in (16) was arbitrarily chosen to be 10^{-4}, and all other parameters except α are from table 1. Under these assumptions, for any given choice of α, equations (5) give $d = (\alpha+0.5)/160$ and equation (2) gives a carrying capacity outside the break region of $K = 149/(\alpha+0.5)$ foxes km^{-2} per year. For example, if we assume that the rabid period lasts an average of 3.8 days, then $d = 0.6$ and $K = 1.5$ foxes km^{-2} outside of the break. If a reduction scheme can reduce the carrying capacity to 0.4 foxes km^{-2} inside the break region well before the epidemic arrives, then $S_b = 0.26$ and figure 6 gives $x_b = 15$. Assuming a diffusion coefficient of 200 km^2 per year, equations (5) give the predicted break

FIGURE 4. The behaviour of the epizootic front when it encounters a break in the susceptible fox population. These plots show (*a*) the susceptible and (*b*) the rabid fox population densities for a sequence of times as the wave approaches the break region, stops and dissipates. They were obtained by solving equations (1) numerically with a carrying capacity of 2 foxes km^{-2} in the region outside the vertical lines and of 0.4 foxes km^{-2} in the region between them. Other values of parameters were taken from table 1. Note that the susceptible population just outside the break remains slightly higher than elsewhere, since few rabid foxes wander into this region from the right. The density of incubating foxes stays essentially proportional to the rabid population (see the discussion in §3 and in Appendix 1): with the parameter values used the incubating fox density is 5.6 times the rabid fox density. The times and distances are normalized values within the computer model.

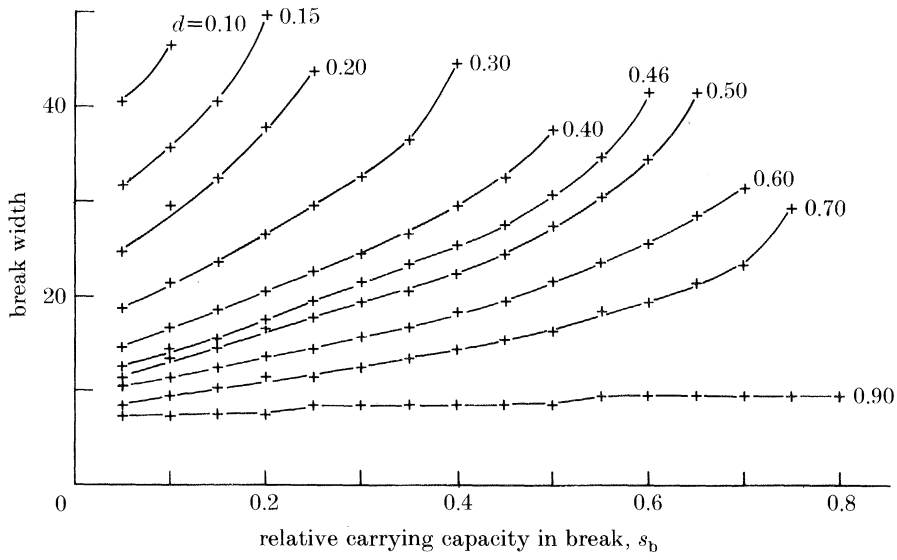

FIGURE 6. The dependence of the break width on the initial susceptible population inside the break, as predicted by the model. The break width, in non-dimensional terms, is plotted against the ratio of the carrying capacity in the break to the carrying capacity outside the break for various values of the duration time of clinical disease, $1/\alpha$ ($d \approx \alpha/\beta K$). These curves were obtained by solving system (1) numerically, until the total infected fox population in the first outbreak is $\frac{1}{2}$ fox km^{-1}. We use the scheme described in the text to calculate this break width, which can be put into dimensional form by using relations (5), i.e. the break width X_c is $(D/\beta K)^{\frac{1}{2}} x_c$, where x_c is the non-dimensional break width with $m = 10^{-4}$. βK was set at 160 per year, and all other parameters, except α, were taken from table 1. For example, if we assume that $1/\alpha = 5$ days then $d = 0.46$ and the carrying capacity outside of the break is 2 foxes km^{-2}. If the carrying capacity inside the break is assumed to be 0.4 foxes km^{-2} then $S_b = 0.2$ and this figure predicts that $x_c = 18$. Assuming that $D = 200$ km^2 yr^{-1}, the predicted break width X_c is 20 km.

width as 17 km. Of course, the choice of p and m depends on how cautious we want to be. The effect on the width of the break for varying p and m is shown in figure 7. Except for p and m, the parameters used in obtaining figure 7 are the same as for the curve $d = 0.46$ in figure 6 ($1/\alpha = 5$ days, $K = 2$ foxes km^{-2} outside the break region). The maximum value of $I+R$ at t_c for all of the calculations was less than 0.15 foxes km^{-2}. Even with $m = 10^{-2}$ there are fewer than 0.0015 infected foxes km^{-2} on the protected side of the break.

We can determine analytically an approximate functional dependence of the break width on the parameters. The behaviour of the various fox population densities in the break region after the epizootic wave has reached it should be similiar to the situation in which a concentrated localized density of infected and rabid foxes at time $t = 0$ (with the same total number of I and R as for the epizootic wave) is introduced at $x = 0$ in a domain where the carrying capacity is everywhere equal to the initial fox density in the break. We can then obtain an estimate of the break width by looking at the following idealized problem. Suppose that the carrying capacity is zero for all x, which implies that the susceptible fox density

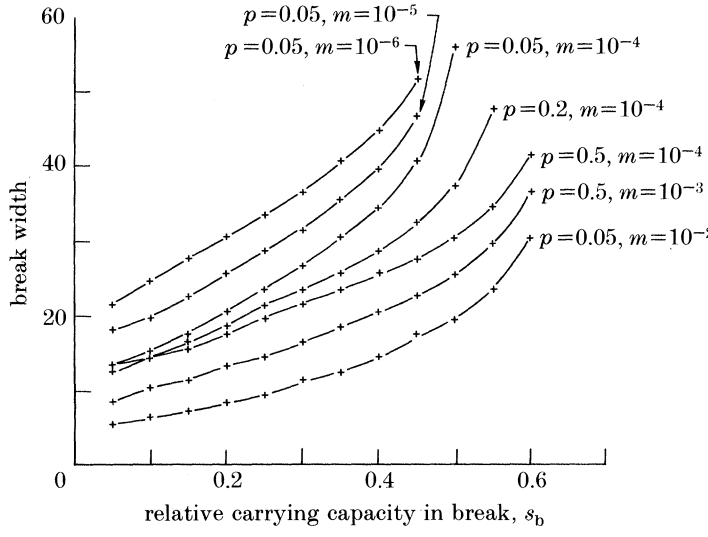

FIGURE 7. The sensitivity of the break width to the parameters used in our scheme for estimating it. As in figure 6, the non-dimensionalized break width is plotted against the relative carrying capacity in the break region, this time for different values of p and m. p is the total infected fox population per kilometre (that is the integral over x of $I+R$), at the time that the epidemic is assumed to be eliminated, and m is the ratio of the infected density at the far edge of the break to that at the leading edge. The break width X_c is $x_c(D/\beta K)^{\frac{1}{2}}$, where x_c is the non-dimensional break width. $K = 2$ foxes km^{-2} outside of the break and all other parameters are taken from table 1 ($d = 0.46$). As would be expected, decreasing either p or m increases the predicted break width.

For example, suppose that the population reduction scheme makes $K = 0.4$ foxes km^{-2} in the break region. Assuming that $D = 200$ km^2 per year and taking $p = \frac{1}{2}$ fox km^{-1}, as m varies from 10^{-2} to 10^{-4} the predicted break width goes from 9 to 20 km.

$s = 0$. At time $t = 0$, take $r = r_0\delta(x)$ and $q = q_0\delta(x)$, where $\delta(x)$ is a Dirac delta function (that is all of the r_0 rabid foxes are concentrated at $x = 0$). From the values in table 1 the dimensionless inverse of the incubation time μ is small compared with d and $1-d$ (see also the discussion in the appendixes) and as a consequence we can determine, with the above scenario, an analytical expression for x_c (see Appendix 2 for details) to first order in μ, ϵ and δ, which are also small. In non-dimensional terms we find

$$x_c \sim (d-\mu)^{-\frac{1}{2}} \ln (1/m). \tag{17}$$

In dimensional terms, from (5), this gives

$$X_c \sim -(\beta K)^{-1}[D(\alpha+b+\sigma)]^{\frac{1}{2}} \ln m, \tag{18}$$

with typical values for these parameters given in table 1.

The dependence of x_c, in (17), on d and m roughly agrees with figures 6 and 7. It also suggests that the break width should not be very sensitive to p, which is so when the carrying capacity in the break is not too close to the critical value.

6. Two-dimensional epizootic fronts and effects of variable fox densities

In general, fox populations are not uniform, but instead vary according to the hospitality of the local environment. In this section we look at what happens when the epizootic wave encounters a localized region of different carrying capacity from the surrounding environment. In two dimensions the diffusion term in system (1) becomes $D(\partial^2 R/\partial X^2 + \partial^2 R/\partial Y^2)$. Suppose that the carrying capacity, K, and the initial susceptible fox density are equal to a uniform value everywhere on a square region, except for a small patch in the centre of the square, where they have different values. We now introduce a distribution of rabid foxes along one edge of the square, so that a one-dimensional epidemic front starts off across the square, and solve the model equations numerically. Figures 8 and 9 respectively show the resulting rabid and susceptible fox population densities for lower and of higher initial densities in the patch.

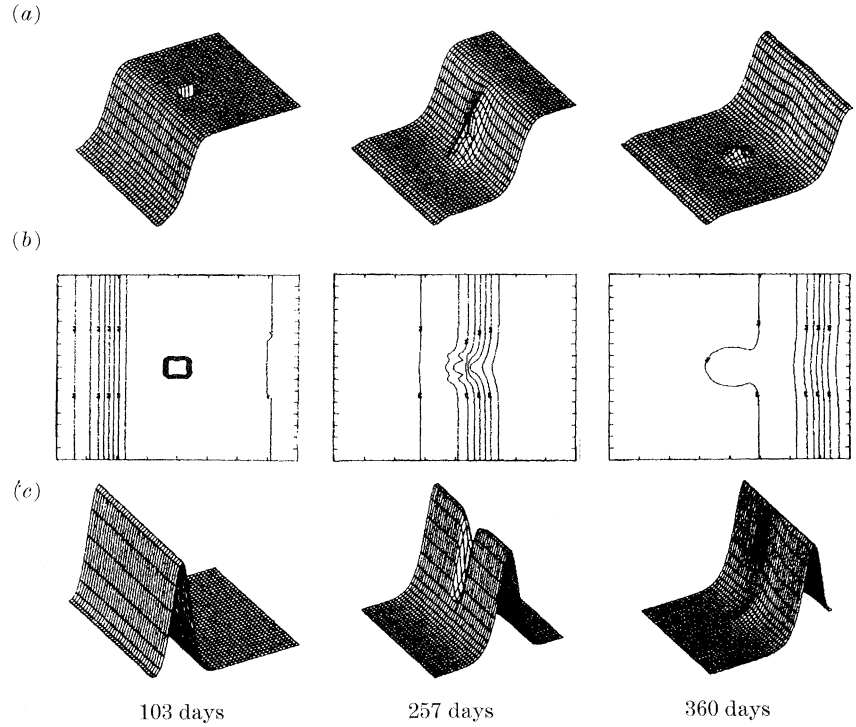

Figure 8. Effect on the epidemic front of a pocket of lowered carrying capacity K. System (1) was solved on a square, with the initial rabies-free fox density and carrying capacity uniform everywhere except in a rectangular region in the centre. In the centre patch K (S_0) is 0.6 of the value outside. The epidemic wave comes in from one side of the square, and travels across. The results are shown for a sequence of three times: before the epidemic reaches the pocket, as the front passes the pocket, and afterward. (*a*) Three-dimensional plot of the susceptible fox population density. (*b*) Contour plot of the susceptible fox density with contour intervals of 0.1 where the density is normalized to run from 0 to 1. (*c*) Three-dimensional plot of the rabid fox density at each point in the square.

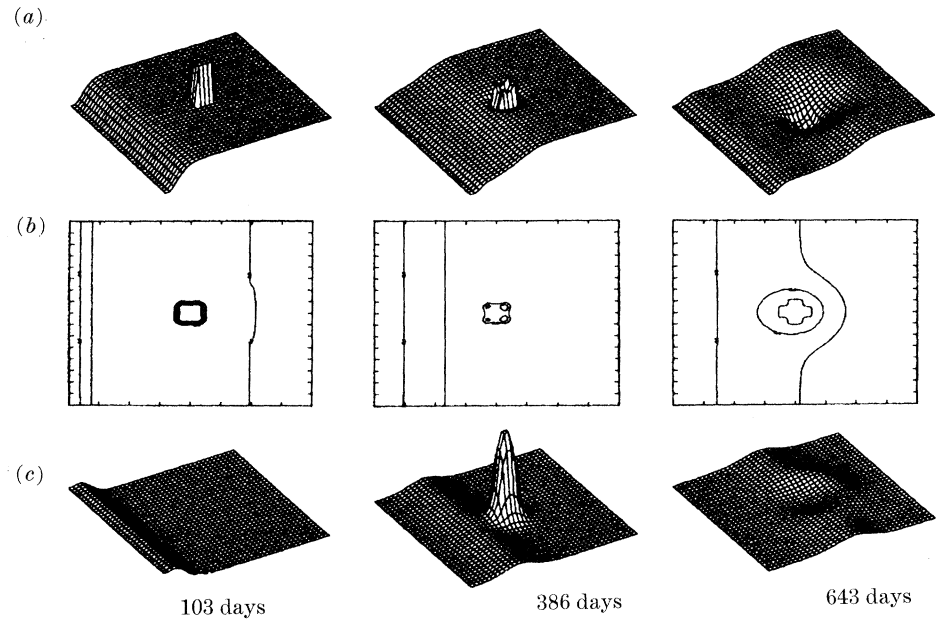

FIGURE 9. Effect on the epidemic front of a pocket of higher initial fox density (and carrying capacity). System (1) was solved on a square, with the initial rabies-free fox density and the carrying capacity uniform everywhere except in a rectangular region in the centre, where they were raised by a factor of 1.7. The results are shown for a sequence of three times: as the wave comes in from one side, as it passes the higher density pocket, and after it passes. (*a*) Three-dimensional plot of the susceptible fox population density. (*b*) Contour plot of the susceptible fox density, with contour intervals of 0.1, where the density is normalized to have a maximum of 1. (*c*) Three-dimensional plot of the rabid fox density at each point in the square.

From figure 8*b* we see that the front moves more slowly through the region of lowered carrying capacity, and from figure 9*b* that the reverse happens for the pocket of raised capacity. The residual fox population, once the first outbreak has moved past, is slightly higher in the pocket of lowered K (and lower in that of raised K), than in the surrounding region. One interesting feature is that the pocket of lowered density provides a sort of protection to the region just adjoining it. There are never as many cases of rabies in a ring around the outside of this region, and the final susceptible population density is higher there than further away. The break region of the previous section also exhibits this feature, which arises because the region of lower density does not provide as many rabid foxes to diffuse into this area – there is, in effect, a preferential direction for the diffusion. The pocket of higher density has the opposite effect. Another interesting fact is that the epidemic appears to jump ahead of the epidemic front into the pocket of higher density (see the central figure in figure 9*c*). This is a focusing effect, which could account for some of the cases when outbreaks of rabies appear in advance of the front.

7. Rabies in England: some quantitative predictions

For some time now, England has remained rabies-free owing mainly to the strict quarantine laws and high public awareness of the potential dangers. With the proximity of the disease in the north of France and the increased private traffic between continental Europe and Britain it seems possible that the disease will be brought into Britain in the near future. The appearance of rabies in Britain is particularly serious because of the high density of foxes, both urban and rural, in England. An additional cause for concern is the apparent compatibility of these urban foxes with cats (Macdonald 1980). If no control measures are applied, the epidemic would move quickly through England. We can use our model to obtain a rough estimate for the position of the epidemic front after rabies is introduced into the fox population.

Macdonald (1980) gives a map of estimated fox densities in England. We covered the lower half of England with a grid, and assigned a density to each square based on the values given on his map. Contour lines of these densities, normalized from 0 to 1, are shown in figure 10. A value of 1 corresponds to 2.4 adult foxes per

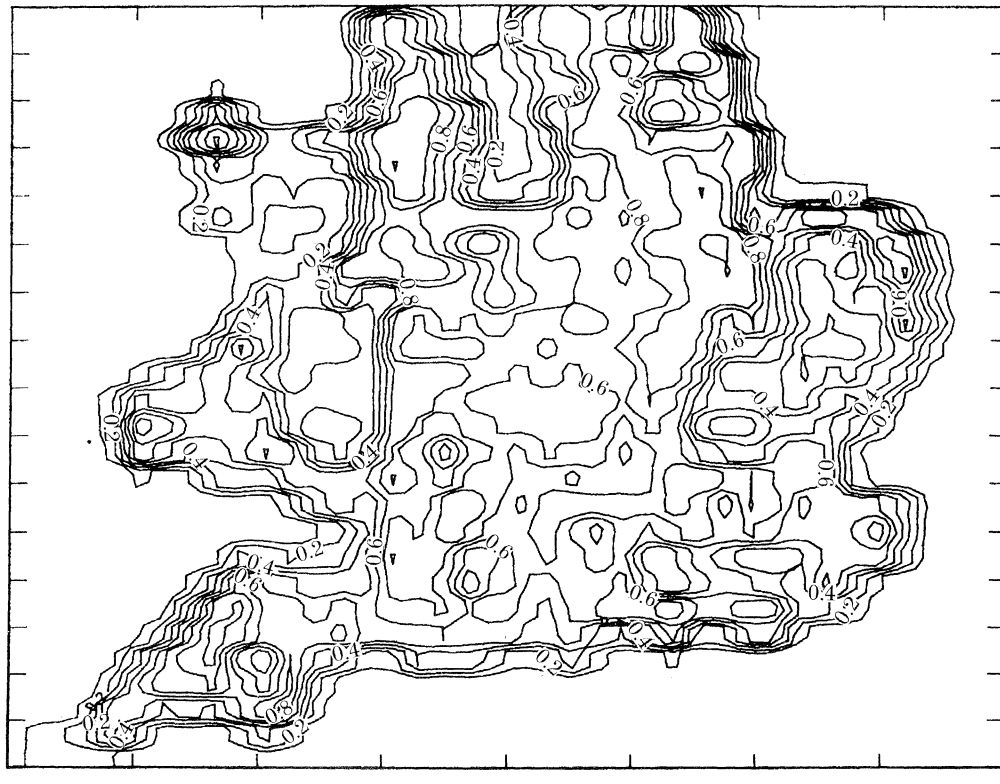

Figure 10. Contour plot of fox densities in the southern half of England that were used in our numerical simulations. Values are scaled to lie between 0 and 1, with 1 corresponding to 2.4 adult foxes km^{-2} in springtime, or to an average of 4.6 foxes km^{-2} throughout the year. These values are based on Macdonald's (1980) estimates, who emphasizes that the density map is probably not very accurate but is based on educated estimates.

square kilometre in springtime. Recall that our model is stated in terms of densities averaged over the yearly cycle (see assumption (i), §2). Before the introduction of rabies, the population increases to its yearly high just after whelping, then gradually returns to the adult springtime population. The average density is roughly the mean between the populations just before and just after whelping. The ratio of males to females is about 1.2:1, and females have an average of 3.7 to 4.2 cubs each year (Lloyd *et al.* 1976). Thus the average population is about 1.9 times the springtime adult population, and 1 corresponds to a carrying capacity of 4.6 foxes km^{-2} in figure 10.

Using the carrying capacities (and initial fox densities) shown in figure 10, and supposing, by way of illustration, that the rabies epidemic starts near Southampton, we solved the two-dimensional form of system (1) numerically. The parameter values given in table 1 were used, and the diffusion coefficient was taken to be 200 km^2 per year. The numerical simulations took about 120 minutes on a Cray XMP-48 at the Los Alamos National Laboratory. The results are shown in figures 11 and 12. The position of the front every 100 days is shown in figure 11. We see that with such high fox densities the epidemic very quickly reaches most of the region studied. Within 4 years the front has effectively reached Manchester. The sequence in figure 12 shows that, just as in the uniform density case, most of the cases of rabies are concentrated in a narrow band at the front; the susceptible population is effectively decimated by the epidemic and regenerates before another

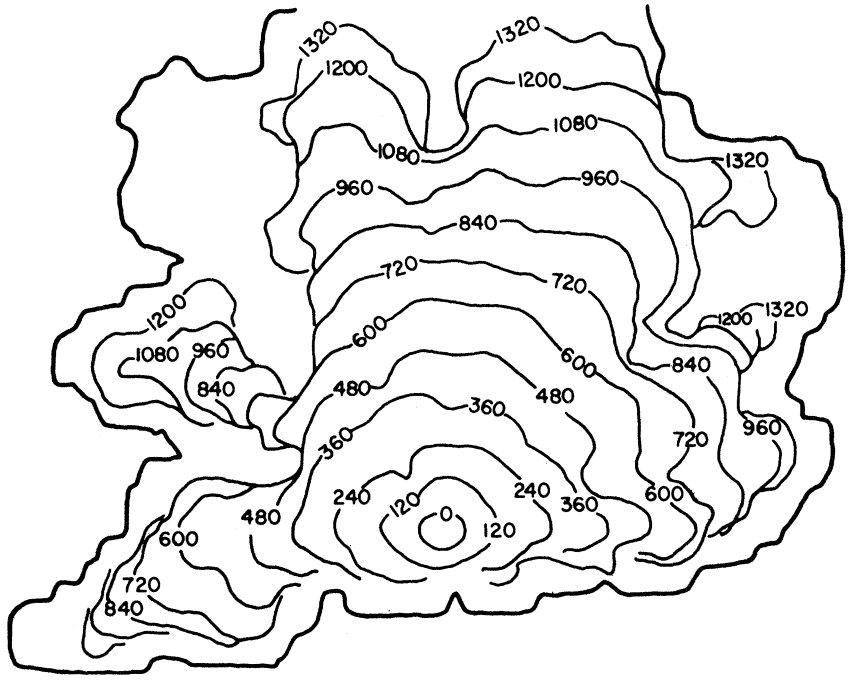

FIGURE 11. The position of the wavefront every 120 days as predicted by our model and the fox densities in figure 10. We assumed a diffusion coefficient of 200 km^2 per year, and took the other parameter values from table 1.

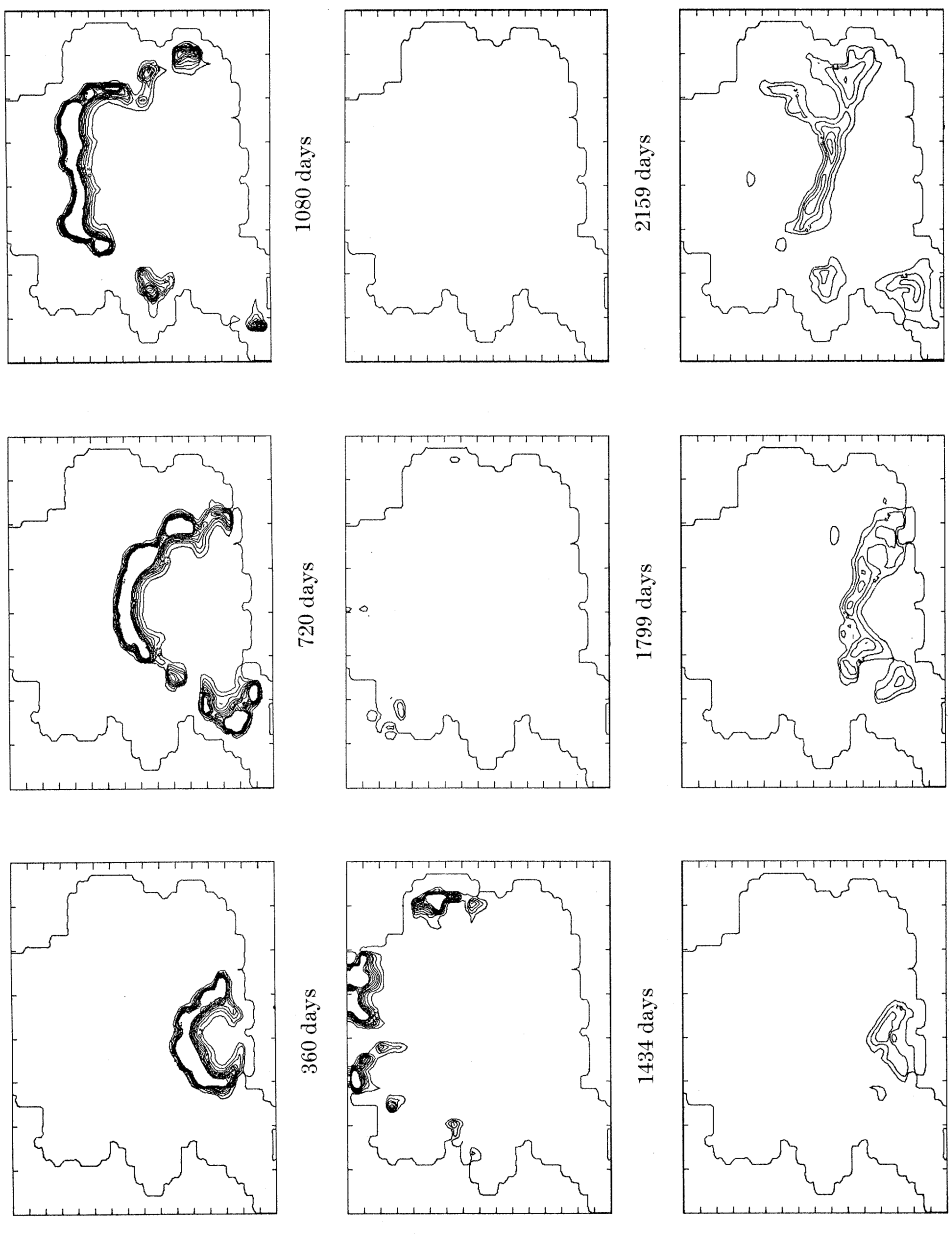

FIGURE 12. The epidemic front as it moves through the southern part of England. This was obtained by solving system (1) numerically, with the local carrying capacities and initial susceptible fox densities shown in figure 10. A localized density of rabid foxes was introduced at Southampton initially, and allowed to spread. Contour plots of the rabid fox densities are given at a sequence of times, as the wave moves outward from its source. Note that, just as in the one-dimensional case, there are few rabid foxes in the region behind the front. Note also the reappearance of

wave starts again. Figure 12 shows the second outbreak starting off from Southampton, about 7 years after the first one.

These quantitative predictions are very rough. Macdonald (1980) emphasizes that the fox densities in his map are only educated guesses, based on his knowledge of fox ecology. As we emphasized in §4, not enough is known about the behaviour of rabid foxes to obtain a sharp estimate for the diffusion coefficient, which means that the speed of the wave may be anywhere from one half to four thirds of our calculated result. We have also neglected such geographical factors as rivers, which tend to provide a channel for the epidemic, speeding its movement parallel to the banks and temporarily halting its direct passage. However, we believe that this relatively simple model provides a plausible quantitative first estimate for the progression of rabies in England if the epidemic wave were allowed to move unchecked. As we saw above, it also gives the break widths that would seriously impede the spread of the disease.

8. Conclusions

We have investigated a simple deterministic model for the spatial spread of the rabies epidemic among foxes, which incorporates many of the salient features of the disease and the ecology of foxes. Our model is sufficiently simple that we could obtain fairly reliable estimates for all of the parameters except the diffusion coefficient, for which we obtained a range of possible values. Analysis of the model produces certain predictions for the behaviour of the epidemic wave, in different environments, which we believe provide some quantitative insight into the spatial spread of the epidemic and the transmission mechanisms responsible for its spread. For example, it is not known whether the primary reason for the spatial spread of the epidemic is the encroachment of confused rabid foxes onto their neighbour's territories, as we have assumed, or the migration of young foxes who carry the disease with them while healthy, or if both mechanisms are equally important. By isolating one of these mechanisms, we can determine how the epidemic wave behaves if that is the primary factor in its spatial spread, and compare the results with observation in continental Europe to see if it is possible for it to be the dominating factor. Our results indicate that the confused movements of rabid foxes is indeed sufficient to account for much of the behaviour of the current epidemic. It would be interesting to investigate a model in which migrating young foxes are the primary cause for spatial spread of rabies.

The agreement of our model with the available epidemiological evidence is quite good, despite the uncertainty in the size of the diffusion coefficient. For an initial fox density of 2 foxes km^{-2}, which is similiar to densities reported for much of mainland Europe, and for any reasonable choice of diffusion coefficient, the speed of the epidemic front (25–65 km per year), obtained from our model, encompasses the range of 30–60 km per year usually observed. The speed of the wave increases with fox density, and drops to zero as the fox density decreases to the critical value. The model also predicts that rabies will essentially disappear for a period of about 5 years after the first outbreak, and then reappear, with the second outbreak weaker than the first. This correlates very well with what has happened in many

parts of Europe. Another interesting feature that emerges from the model is the enhanced movement of the rabies epidemic into regions of higher density *in advance of* the rest of the front. This may help to explain why outbreaks seemingly far in advance of the epidemic occasionally occur.

It is possible for a strip of lowered susceptible fox population to check the progression of the epidemic, and protect an uninfected region ahead of the front. For this method of control to be efficiently applied, it is essential to have an indication of how wide an effective break region must be. For our model control scheme, figure 6 shows non-dimensional estimates for this width. If there are 2 foxes km^{-2} initially, and the reduction scheme is 80 % effective, then figure 6 gives a break width of 10–25 km, depending on the diffusion coefficient. This is of the right order of magnitude when compared with the protective break that has proved effective in Denmark, where intensive control measures were applied to a strip 20 km wide with less intensive measures used in an adjoining 20 km strip.

The probability that rabies will eventually reach England and other uninfected regions is high. It is clearly of considerable importance to understand as much as possible about the disease, its transmission and how it spreads, well before it arrives. The density of foxes in England is much greater in many areas than on the continent, and the epidemic may proceed differently there. Figures 11–12 summarize some of our model's predictions for a particular choice of diffusion coefficient, and some estimates for the current fox populations in the southern half of England. Perhaps the most disturbing aspect of these results is the rapidity with which the epidemic would move through the central region, namely at speeds of around 100 km per year. No less disturbing is the reappearance of the disease several years after the passage of the epidemic front, a fact that could well give rise to complacency.

J.D.M. thanks the Los Alamos National Laboratory, Los Alamos, New Mexico, where most of this work was performed during a visit in 1985 as the Stan Ulam Visiting Scholar.

Appendix 1. Mathematical analysis of travelling epizootic waves

1. *Linear analysis and wave speed determination*

We look for epizootic wave solutions to the dimensionless system (6), which travel at a constant velocity v into an undisturbed, rabies-free region. We thus look for solutions s, q and r as functions of the single variable $\xi = x+vt$ that satisfy

$$\left.\begin{aligned} vs' &= \epsilon(1-n)\, s - rs, \\ vq' &= rs - (\mu+\delta+\epsilon n)\, q, \\ vr' &= \mu q - (d+\epsilon n)\, r + \mathrm{d}^2 r/\mathrm{d}\xi^2, \\ n &= s+q+r, \end{aligned}\right\} \tag{A1.1}$$

where prime denotes differentiation with respect to ξ, and where $s \to 1$, $q \to 0$, $r \to 0$ as $\xi \to -\infty$, that is far ahead of the wave front. Physically, none of the population densities can be negative, so we are interested only in non-negative solutions.

Practical values of the model parameters make $\epsilon \ll 1$ and $\delta \ll 1$, which suggests an asymptotic analytical procedure.

The system (A 1.1) has three possible steady-state solutions in the positive quadrant: $(s, q, r) = (1, 0, 0)$, $(0, 0, 0)$ and (s_0, q_0, r_0), where s_0, q_0 and r_0 are given, up to first order in ϵ and δ, by

$$s_0 = d + [\epsilon + (\epsilon d + \delta)/\mu]\, d, \quad q_0 = \epsilon d(1-d)/\mu, \quad r_0 = \epsilon(1-d). \tag{A 1.2}$$

From the full expressions for (s_0, q_0, r_0) all of s_0, q_0 and r_0 are non-negative only if

$$0 < d < [1 + (\epsilon + \delta)/\mu]^{-1} - \epsilon. \tag{A 1.3}$$

If a travelling wave solution to the system (6) exists that has the required properties, it will appear as a trajectory, in the phase space of (A 1.1), which goes from the equilibrium at $s = 1, q = r = 0$ to one of the other two equilibrium points, $(0, 0, 0)$ or (s_0, q_0, r_0), and remains in the positive quadrant.

Writing (A 1.1) as a first-order system and linearizing about the critical point $(s, q, r, \mathrm{d}r/\mathrm{d}\xi) = (1, 0, 0, 0)$ gives a linear system whose solutions are linear combinations of the eigensolutions $x_i \exp(\lambda_i \xi)$ where x_i and λ_i are the four eigenvectors and eigenvalues of the coefficient matrix. Sufficiently close to the critical point, solutions of (A 1.1) follow those of the linearized form. So we can determine the solution behaviour near the critical point by looking at all possible linear combinations of the eigensolutions. If $\mathrm{Re}\,\lambda_i < 0$, then $x_i \exp(\lambda_i \xi) \to 0$ as $\xi \to \infty$ and the trajectory approaches the critical point, whereas if $\mathrm{Re}\,\lambda_i < 0$ the trajectory comes out of the critical point. Trajectories leaving the critical point thus correspond to linear combinations of those eigensolutions with $\mathrm{Re}\,\lambda_i > 0$. If an eigenvalue is complex, then its eigensolution is oscillatory.

The four eigenvalues for the linear system near $(1, 0, 0, 0)$ are $\lambda = -\epsilon/v < 0$ and the roots of the cubic

$$f(\lambda) = \lambda^3 + [(\mu + \delta + \epsilon)/v - v)]\, \lambda^2 - (d + \mu + \delta + 2\epsilon)\lambda + [\mu(1 - d - \epsilon) - (\delta + \epsilon)(d + \epsilon)]/v. \tag{A 1.4}$$

$f(\lambda) \to \infty$ as $\lambda \to \infty$ and $f(\lambda) \to -\infty$ as $\lambda \to -\infty$. If (A 1.3) holds, then $f(0) > 0$ and f has a negative slope at $\lambda = 0$. Depending on the values of the various parameters, f can look like either of the forms illustrated in figure A 1.1.

With all the parameters fixed, as the velocity v is varied f will sequentially look like each of these shapes. Thus, as long as (A 1.3) holds f has one negative real root and, depending on the value of the velocity of the wave, it has either two positive real roots or two complex roots. When the velocity is such that the roots of (A 1.4) are complex, with $\mathrm{Im}\,\lambda \neq 0$, these represent oscillatory solutions, which imply negative populations, and hence physical waves cannot travel with such velocities. The bifurcation value for v, v_c say, between realistic and unrealistic solutions is the value when (A 1.4) has a double root. Thus the range of velocities is determined by finding v_c. This is given by setting $f = 0$ and $\mathrm{d}f/\mathrm{d}\lambda = 0$ and eliminating λ, to get an equation for v_c in terms of the parameters. To first order in ϵ and δ it is given by the positive real roots of $g(v_c^2)$, where $g(z)$ is given by

$$g(z) = [4\mu + (d-\mu)^2]\, z^3 + 2[3\mu(1-d)(3d+\mu) + (d+\mu)^2(2d+\mu)]\, z^2 + \mu^2[(d+\mu)^2 - 6(1-d)(3d+\mu) - 27(1-d)^2]\, z - 4\mu^4(1-d), \tag{A 1.5}$$

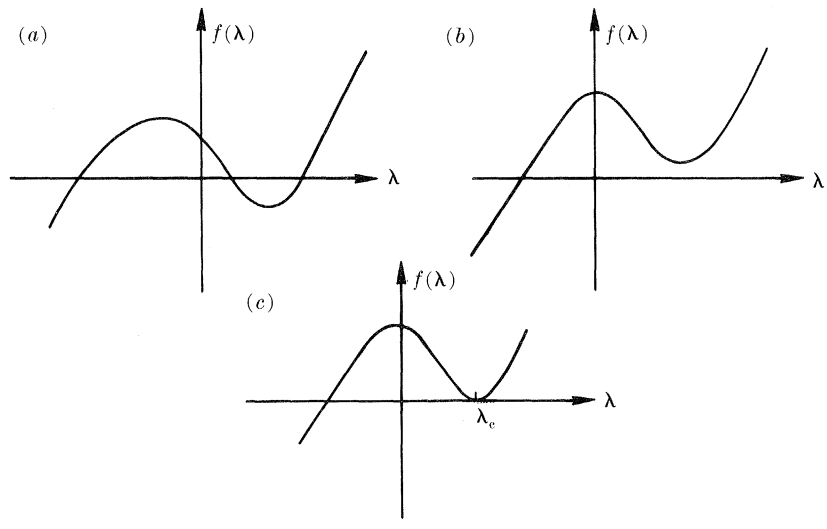

FIGURE A1.1. The eigenfunction cubic (A1.4) may have two positive roots (*a*) or none (*b*). λ_c is the critical (double) root situation (*c*).

which is equation (9) in the paper. $g(z)$ is negative and $\mathrm{d}^2g/\mathrm{d}z^2$ is positive at $z = 0$ when (A1.3) holds. A rough sketch of $g(z)$ shows it has a unique positive root that corresponds to the minimum possible velocity for an epizootic wave.

We now show that it is not possible for a trajectory to go from the critical point at $s = 1$ to that at the origin. On linearizing (A1.1) about the origin we find the eigensolutions

$$\begin{bmatrix} s \\ q \\ r \\ r' \end{bmatrix} = \boldsymbol{a} \exp[-(\mu+\delta)\xi/v], \quad \boldsymbol{b} \exp[\tfrac{1}{2}v \pm (d+\tfrac{1}{4}v^2)^{\frac{1}{2}}]\,\xi, \quad \boldsymbol{c} \exp[\epsilon\xi/v],$$

where

$$\boldsymbol{a}^{\mathrm{T}} = [0,\ (d-\mu-\delta)/\mu - (\mu+\delta)^2/\mu v^2,\ 1,\ -(\mu+\delta)/v],$$

$$\boldsymbol{b}^{\mathrm{T}} = [0,\ 0,\ 1,\ \tfrac{1}{2}v \pm (d+\tfrac{1}{4}v^2)^{\frac{1}{2}}], \quad \boldsymbol{c}^{\mathrm{T}} = [1,\ 0,\ 0,\ 0],$$

and where the superscript T denotes the transpose. Sufficiently close to the origin, trajectories that approach the origin are linear combinations of the two eigensolutions with negative exponents, and so they approach the origin in the plane $s = 0$. For the system (A1.1) 'time' is reversible, in the sense that we can replace ξ by $-\xi$ and trace backwards along any trajectory. Setting $\tau = -\xi$ in (A1.1) and taking $s = 0$ initially, we see that $s = 0$ for all positive τ irrespective of the initial values of r and q. This implies that a trajectory that has $s = 0$ for any ξ had $s = 0$ for all previous ξ, and has $s = 0$ for all subsequent ξ. So a trajectory cannot come from $s = 1$, enter the $s = 0$ plane, and approach the origin.

This implies that a travelling wave can only occur if there is a trajectory from $s = 1$ to the critical point (s_0, q_0, r_0) and therefore that condition (A1.3) must hold.

To determine the behaviour of the wave as it approaches this critical point, we now linearize (A1.1) about (s_0, q_0, r_0) to get, after some algebra, the eigenvalues

$$\lambda_1, \lambda_2 = \tfrac{1}{2}[v-\mu/v \pm \{(v-\mu/v)^2+4(\mu+d)\}^{\frac{1}{2}} \tag{A1.6}$$

to first order in ϵ and δ, and

$$\lambda_3, \lambda_4 = \{\pm \mathrm{i}[\epsilon\mu d(1-d)/(\mu+d)]^{\frac{1}{2}}/v\} - \epsilon d[2v(\mu+d)^2]^{-1}[\mu(1-d)(\mu/v^2-1)+(\mu+d)^2] \tag{A1.7}$$

to second order in ϵ and δ. λ_1 is positive, and so, near the critical point, any solution that approaches (s_0, q_0, r_0) as $\xi \to \infty$ is a linear combination of the eigensolutions corresponding to λ_2, λ_3 and λ_4. Since $|\lambda_2| \gg |\mathrm{Re}(\lambda_3, \lambda_4)|$, the amplitude of its eigensolution decays much more rapidly than that of the eigensolutions of the complex eigenvalues. Thus sufficiently far back in the tail of the wave (that is for sufficiently large ξ), it is the solutions corresponding to the complex eigenvalues that govern the behaviour of the travelling wave. The eigenvectors corresponding to these eigenvalues are given by

$$\begin{bmatrix} s-s_0 \\ q-q_0 \\ r-r_0 \\ r' \end{bmatrix} = \begin{bmatrix} 1 \\ \pm \mathrm{i}[\epsilon d(1-d)/\mu(\mu+d)]^{\frac{1}{2}} \\ \pm \mathrm{i}[\epsilon\mu(1-d)/d(\mu+d)]^{\frac{1}{2}} \\ \epsilon\mu(1-d)/v(\mu+d) \end{bmatrix},$$

which on taking an arbitrary real linear combination of the eigensolutions, gives for sufficiently large ξ

$$\left.\begin{aligned} s-s_0 &\sim [A\cos\omega\xi/v + B\sin\omega\xi/v]\exp(-\lambda\xi/v), \\ q-q_0 &\sim (\omega/\mu)[A\sin\omega\xi/v - B\cos\omega\xi/v]\exp(-\lambda\xi/v), \\ r-r_0 &\sim (\omega/d)[A\sin\omega\xi/v - B\cos\omega\xi/v]\exp(-\lambda\xi/v). \end{aligned}\right\} \tag{A1.8}$$

Here ω is the period of the waves, given by the imaginary part of the complex eigenvalues divided by v, and λ is the decay rate of the amplitude, given by the real part of these eigenvalues divided by v. A and B are constants, which depend on the way the trajectory approaches s_0, q_0, r_0 and cannot be determined from a linear analysis.

2. *Scaling arguments, nonlinear analysis and estimates for the maximum number of rabid foxes during the epizootic*

From (A1.2) and (A1.8) we then have $q \sim rd/\mu$ for sufficiently large ξ: that is the profiles for the infected and rabid fox densities are similar, differing only in scale. In the simulations of the full nonlinear system, the striking profile similarity holds for the *entire* wave, as is seen from figures 1 and 2. This surprising fact suggests that, in view of the complexity of the three-species model, it would be of interest and considerable benefit to investigate analytically the conditions under which we could replace the three-species model with a two-species model; that is we could replace, for example, a susceptible, infected and rabid system, by a susceptible, rabid fox system: the infected fox population is then given by a simple

scaling of the rabid population, which of course would have to be determined. Under certain conditions, it is possible to give an analytical explanation of why this phenomenon occurs: it is not completely obvious from the model system (A 1.1).

A crucial first step is to note that for both sets of parameter values used in the numerical simulations the parameters d and μ satisfy $d \gg \mu$ and $(1-d) \gg \mu$ (μ was 0.08 and 0.04), whereas the non-dimensional velocity v is about the same size as d. Furthermore, ϵ and δ are about the same size as μ^2. If we assume that these order-of-magnitude comparisons hold in general, that is

$$\left.\begin{aligned} &0 < \mu \ll 1, \quad 0 < \epsilon = \mu^2 \epsilon_0, \quad 0 < \delta = \mu^2 \delta_0, \\ \text{and} \qquad &d,\ 1-d,\ v,\ \epsilon_0,\ \delta_0 \text{ are all } O(1), \end{aligned}\right\} \tag{A 1.9}$$

we can use a singular perturbation analysis (see, for example, Murray 1984) to obtain asymptotic solutions to the full nonlinear system (A 1.1) in the limit as $\mu \to 0$. The technical mathematical details will be presented elsewhere but here we give a brief account of the arguments as to why r and q have similar profiles.

To show that r and q have similar profiles we need only show their similar dependence on s, that is the curves $q(s)$ and $r(s)$ should differ only in scale. Using the chain rule expressions

$$\left.\begin{aligned} r' &= s'\, \mathrm{d}r/\mathrm{d}s, \\ r'' &= s'\, \mathrm{d}(s'\, \mathrm{d}r/\mathrm{d}s)/\mathrm{d}s = s'\{s'\, \mathrm{d}^2 r/\mathrm{d}s^2 + (\mathrm{d}s'/\mathrm{d}s)\,(\mathrm{d}r/\mathrm{d}s)\} \end{aligned}\right\} \tag{A 1.10}$$

with similar ones for q, where prime denotes differentiation with respect to ξ, we can replace the q and r equations in (A 1.1) by equations that involve s as the independent variable rather than ξ. Further, from the numerical solutions in figures 1 and 2, r is everywhere very much smaller than q. In fact specifically from (A 1.8) we see that asymptotically $q - q_0 \sim d(r - r_0)/\mu$. This suggests that we should introduce a new stretched variable y for the rabid population by setting

$$r(s) = \mu y(s),$$

where we expect y, as well as q, to be $O(1)$. Using (A 1.10) in the q and r equations in (A 1.1), together with the first of (A 1.1) to replace s' with its right-hand side, and the last transformation, we obtain the following (travelling wave) phase plane equations for q and y with s as the independent variable:

$$\left.\begin{aligned} &[-ys + \mu\epsilon_0 s(1-n)]\, \mathrm{d}q/\mathrm{d}s = ys - q - \mu(\delta_0 + \epsilon_0 n)\, q, \\ q - dy = {} &\mu[-ys + \mu\epsilon_0 s(1-n)]\, \mathrm{d}y/\mathrm{d}s - \mu^2 v^{-2}[-ys + \mu\epsilon_0 s(1-n)] \\ &\times \{[-ys + \mu\epsilon_0 s(1-n)]\, \mathrm{d}^2 y/\mathrm{d}s^2 + [-y + \mu\epsilon_0(1-n-s) - s(1+\mu^2\epsilon_0)\, \mathrm{d}y/\mathrm{d}s \\ &- \mu\epsilon_0 s - \mu\epsilon_0 s\, \mathrm{d}q/\mathrm{d}s]\, \mathrm{d}y/\mathrm{d}s\} + \mu^2 \epsilon_0 yn, \\ &n = s + q + \mu y. \end{aligned}\right\} \tag{A 1.11}$$

These are the equations we now consider in detail to show that q is proportional to y (and hence r) over the complete travelling wave domain in s, and hence in the travelling wave coordinate $\zeta = x + vt$.

We know from the last section that the solution trajectory of interest starts at $s = 1, q = y = 0$ and eventually spirals into $s_0 \sim d, q_0 \sim \mu\epsilon_0 d(1-d), y_0 \sim \mu\epsilon_0(1-d)$. Note also, from (A 1.11), that for small μ, $\mathrm{d}s/\mathrm{d}y \approx 0$ for $y = \mu\epsilon_0(1-n) = O(\mu)$. So, with the knowledge we now have of the solution trajectory in the y–s plane, it is qualitatively as illustrated in figure A 1.2, with the bottom parts of the successive loops approximately straight lines parallel to the s-axis.

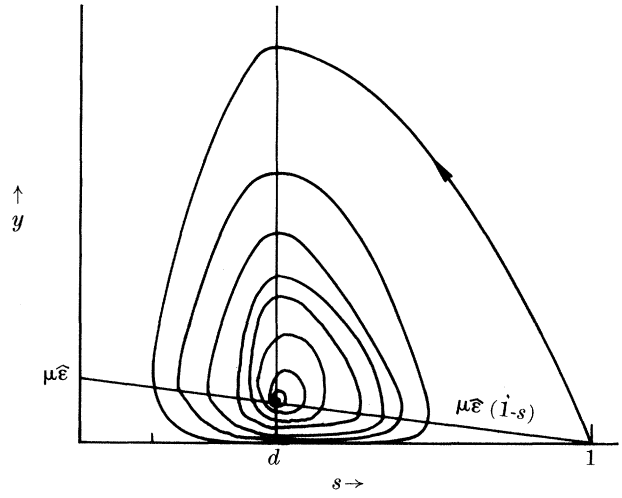

FIGURE A 1.2. Schematic phase plane solution trajectory for the scaled rabid population y in terms of the susceptible population s, from (A 1.11).

To show the trajectory similarity between q and y we must now be more precise. The first few loops of the spiral-type trajectory in figure A 1.2 are each made up of four main pieces, which are schematically illustrated in figure A 1.3*a–d*. These consist of the top (*a*), where y and q are $O(1)$ and the s-variation is $O(1)$, the left (*b*) and right (*c*) corners where y and q are $O(\mu)$, and s is respectively near a value s_{L} and s_{R} say, and the bottom of the curve, where y and q are even smaller than μ, and s varies by $O(1)$. The equations governing the solution in these different regions take on different approximate forms, the solutions of which have to be matched in a singular perturbation way. The full analysis will be omitted here but the procedure is described with sufficient detail to demonstrate the main point, namely that q is directly proportional to r.

For the upper part of the curve, that is figure A 1.3*a*, both y and q are $O(1)$. We expect terms multiplied by μ in (A 1.11) to be negligible, and so here the solution behaviour is governed by

$$-ys\ \mathrm{d}q/\mathrm{d}s = ys - q, \quad q - dy = 0,$$

the solution of which is

$$y(s) = \ln(s/s^*) + (s^* - s)/d, \quad q(s) = dy(s), \tag{A 1.12}$$

where s^* is a constant of integration. Note that over this part of the solution trajectory the infected population q is proportional to the rabid population y, as we wished to show. The solution $y(s)$ here has two zeros, s_{L} and s_{R} say, where

$$0 \leqslant s_{\mathrm{L}} < d < s_{\mathrm{R}} \leqslant 1. \tag{A 1.13}$$

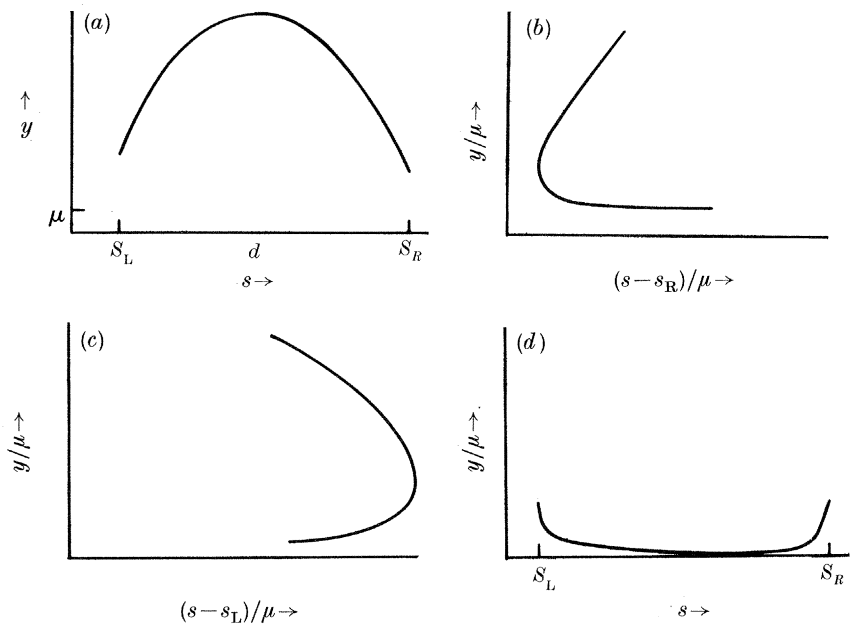

FIGURE A1.3. (*a*) Typical upper part of the y-trajectory where $y = O(1)$ and s varies by $O(1)$. (*b*, *c*) Left and right lower corners of the trajectory where $y = O(\mu)$ and s is approximately constant. (*d*) The bottom part of the curve where $y = o(\mu)$ and s varies by $O(1)$.

These zeros define the positions of the left and right corners of each loop. Of course this solution is only valid as long as the neglected terms are very much smaller than those retained.

If we consider the first loop, then $s_R = 1$. Except for the first loop, as s tends toward either s_L or s_R the term $\mu s(1-n)$ in the first equation is no longer small compared with $-ys$. For the first loop this is also the case as $s \to s_L$ but is not true at the right-hand root, where $1-n$ and y go to zero together. Note that for the first loop (A1.12) becomes

$$y \sim \ln(s) + (1-s)/d \Rightarrow y_{\max} = \ln(d) + (1-d)/d \quad \text{at } s = d. \tag{A1.14}$$

This is a particularly useful result because it allows us to give estimates for the *maximum number of rabid and incubating foxes* during the passage of the epizootic wave. From (A1.12) and the definition of y, using (A1.14), we get

$$r_{\max} \sim \mu[\ln(d) + (1-d)/d], \quad q_{\max} \sim d[\ln(d) + (1-d)/d], \tag{A1.15}$$

which occurs when the susceptible population is $s = d$.

For the corner regions where y, q and $s-s_L$ or $s-s_R$ are all $O(\mu)$, we must introduce a further stretching transformation, namely

$$y_c = y/\mu, \quad q_c = q/\mu, \quad s_c = (s-s^*)/\mu, \quad \text{for } s^* = s_L, s_R. \tag{A1.16}$$

Then (A 1.11) becomes, for $0 < \mu \ll 1$,

$$\left.\begin{aligned}[(s^*+\mu s_c)\,(-y_c+\epsilon_0(1-n)]\,\mathrm{d}q_c/\mathrm{d}s_c &= y_c(s^*+\mu s_c)-q_c-\mu(\delta_0+\epsilon_0 n)\,q_c,\\ q_c-dy_c &= \mu(s^*+\mu s_c)\,[-y_c+\epsilon_0(1-n)]\,\mathrm{d}y_c/\mathrm{d}s_c+O(\mu^2),\\ n &= s^*+\mu(s_c+q_c)+\mu^2 y_c.\end{aligned}\right\} \tag{A 1.17}$$

Now let $\mu \to 0$ in the usual singular perturbation way and the last two differential equations become

$$\left.\begin{aligned}[-y_c+\epsilon_0(1-s^*)]\,s^*\,\mathrm{d}q_c/\mathrm{d}s_c &= y_c s^*-q_c,\\ q_c &= dy_c,\end{aligned}\right\} \tag{A 1.18}$$

the (implicit) solution of which is

$$\left.\begin{aligned}s_c &= ds^*(s^*-d)^{-1}[\epsilon_0(1-s^*)\,\ln y_c-y_c+C],\\ q_c &= dy_c,\end{aligned}\right\} \tag{A 1.19}$$

where C is an integration constant. Once again q is proportional to r to first order in μ.

This corner analysis breaks down when s_c becomes unbounded as we leave the vicinity of the corners. In singular perturbation parlance as $s_c \to \pm\infty$ we have to match the corner solution to the other parts of the solution, specifically the top and bottom part of the trajectory loops in figure A 1.3*a*, *d*. Here as $y_c \to 0$, $\ln y_c \to -\infty$ and $s_c \to +\infty$ for the left corner, $s_c \to -\infty$ for the right corner, as the bottom part of the loop is approached. As $y_c \to +\infty$, once again $s_c \to \pm\infty$ for the left and right corners respectively and the top part of the loop is approached. So, this is saying that as y and q get either large or small, s is no longer close to s^* and some of the neglected terms in (A 1.17) become important.

Finally let us consider the bottom region. Here we make a further stretching transformation by writing

$$y = \nu(\mu)\,y_b, \quad q = \nu(\mu)\,q_b, \quad \text{where } \nu(\mu) = o(\mu), \tag{A 1.20}$$

where for our purposes the specific form of $\nu(\mu)$ need not be determined. The system (A 1.11) with this transformation becomes

$$\left.\begin{aligned}s[\nu y_b+\mu\epsilon_0(1-n)]\,\mathrm{d}q_b/\mathrm{d}s &= y_b s-q_b-\mu(\delta_0+\epsilon_0 n)\,q_b,\\ q_b-dy_b &= \mu s[\nu y_b+\mu\epsilon_0(1-n)]\,\mathrm{d}y_b/\mathrm{d}s+O(\mu^3),\\ \nu &= s+\nu(q_b+\mu y_b).\end{aligned}\right\} \tag{A 1.21}$$

Here we have to be a little more careful in deriving the relevant equation for small μ. From the second of (A 1.21) we again have

$$q_b = dy_b. \tag{A 1.22}$$

The realistic limiting form of the first equation is

$$\mu\epsilon_0 s(1-s)\,\mathrm{d}q_b/\mathrm{d}s = y_b s-q_b,$$

the solution of which gives, with (A 1.22),

$$y_b(s) = A[1/(1-s)]^{(1-d)/\mu\epsilon_0 d}(1/s)^{1/\mu\epsilon_0 d}, \tag{A 1.23}$$

where A is an integration constant. Now, in this part of the curve, y is everywhere $o(\mu)$ by virtue of the transformation (A 1.20). Since $s < 1$ for all but the first loop, this means that as $\mu \to 0$ in (A 1.23), y_b will become unbounded. This solution has to match the corner solutions near s_L and s_R. The only way this can be done is if A is chosen so that (A 1.23) gives such bounded solutions. Thus the appropriate form of (A 1.23) is

$$y_b(s) = C[(1-s_L)/(1-s)]^{(1-d)/\mu\epsilon_0 d}(s_L/s)^{1/\mu\epsilon_0 d}, \tag{A 1.24}$$

where C is another constant available for matching. From the corner transformation (A 1.16), where $y_c = y/\mu$ is $O(1)$, we can plausibly expect C to be $O(\mu/\nu(\mu))$. The detailed analysis in fact determines $C = \mu/\nu(\mu)$.

The complete solution can be constructed by a systematic singular perturbation analysis by appropriate asymptotic matching of the solution for each part of the loop: the analysis is not trivial and is of intrinsic interest. The important point to note is that we have demonstrated that all around the spiralling loops

$$q = dy = dr/\mu \tag{A 1.25}$$

to first order in μ, where $0 < \mu \ll 1$. This is what is observed in the numerical solution of the original system, equations (6), namely figures 1 and 2. As the curves, in travelling wave coordinates, approach the critical point, the linearized system takes over, and the curves are then described by (A 1.6), where, of course, $q = dr/\mu$ still holds. Thus we suggest that *the number of rabid foxes will essentially be proportional to the number of infected foxes at all points on the travelling wave* with (A 1.25) governing the behaviour at all times.

Appendix 2. Mathematical estimate of the break width

In this appendix the mathematical arguments that result in the analytical estimate for the break width given in (17) are presented briefly. As discussed in §5 above, an estimate for the break width can be obtained by assuming that for $x \geqslant 0$, all of the susceptible foxes have been eliminated, for example by immunization or killing. In our analysis here we shall make the added approximation that the nonlinear terms in the equations for the incubating and rabid foxes can be neglected. Since ϵ and δ are small parameters, this should be a reasonable approximation. A further justification for these approximations comes from the numerical computations of the break width, where we found that the computed break width did not change if these terms were neglected. With these assumptions, equations (6) reduce to

$$\left.\begin{aligned} \partial q(x, t)/\partial t &= \mu q(x, t), \\ \partial r(x, t)/\partial t &= \mu q(x, t) - dr(x, t) + \partial^2 r(x,t)/\partial x^2. \end{aligned}\right\} \tag{A 2.1}$$

By symmetry, instead of considering the problem of a δ-function source of infected

foxes at $x = 0$ and $t = 0$ that then move into the region $x \geqslant 0$, the initial conditions can be replaced by

$$q(x, 0) = 2q_0\delta(x), \quad r(x, 0) = 2r_0\delta(x) \tag{A2.2}$$

and the region $-\infty < x < \infty$ considered instead. Here $\delta(x)$ is the Dirac δ-function. The propagation of infected foxes into the break is described by (A2.1) and (A2.2). The quantities of interest, however, are the time t_c at which the population in the break has decayed to a given level, p, defined implicitly by the formula

$$(KD/\beta)^{\frac{1}{2}} \int_0^\infty [q(x, t_c) + r(x, t_c)]\, \mathrm{d}x = p \tag{A2.3}$$

and the break width, x_c, which as discussed in §5 is given implicitly by

$$q(x_c, t_c) + r(x_c, t_c) = m[q(0, t_c) + r(0, t_c)]. \tag{A2.4}$$

First we estimate t_c. Integrating equations (A2.1) with respect to x from 0 to ∞, we get the two ordinary differential equations

$$\left.\begin{aligned} \mathrm{d}Q^*(t)/\mathrm{d}t &= \mu Q^*(t), \\ \mathrm{d}F^*(t)/\mathrm{d}t &= -dF^*(t) + dQ^*(t), \end{aligned}\right\} \tag{A2.5}$$

where

$$Q^*(t) = \int_0^\infty q(x, t)\, \mathrm{d}x, \quad F^*(t) = \int_0^\infty [q(x, t) + r(x, t)]\, \mathrm{d}x.$$

The initial conditions for (A2.5) are $F^*(0) = q_0 + r_0$, $Q^*(0) = q_0$. The first of equations (A2.5) is easily solved for $Q^*(t)$. Q^* can then be eliminated from the second equation, to obtain the following equation for F^*, the (scaled) total number of foxes present in the region $x > 0$:

$$\mathrm{d}F^*/\mathrm{d}t = -dF^* + dq_0 \mathrm{e}^{-\mu t}. \tag{A2.6}$$

With the given initial conditions, the solution to (A2.6) is

$$F^*(t) = [q_0 + r_0 - d/(d-\mu)]\, \mathrm{e}^{-dt} + dq_0 \mathrm{e}^{-\mu t}/(d-\mu). \tag{A2.7}$$

The critical time t_c can then be determined from (A2.3) by solving the equation

$$F^*(t_c) = p(\beta/KD)^{\frac{1}{2}}.$$

Note that each of the two terms on the right-hand side of (A2.7) involves an exponential factor. Since, the reasonable values of the field parameters, $d > \mu$ and $d - \mu = o(1/t_c)$, the first of those terms can be neglected in comparison with the second if t_c is sufficiently large. We shall assume that this is the case, and verify it *a posteriori*. So neglecting the first term, the resulting algebraic equation can be solved to give

$$t_c \sim \mu^{-1} \ln \{d(KD/\beta)^{\frac{1}{2}}\, q_0/[p(d-\mu)]\}. \tag{A2.8}$$

Typical values for d and μ are 0.46 and 0.08, respectively. $(KD/\beta)^{\frac{1}{2}}\, q_0$ can be

approximated from figure 5 and the results of Appendix 1, §2. From the latter, $q \approx dr/\mu$, so that the total number of infected foxes satisfies

$$\int_{-\infty}^{\infty} (I+R)\,\mathrm{d}X = (KD/\beta)^{\frac{1}{2}}(1+\mu/d)\,q_0.$$

From figure 5,

$$\int_{-\infty}^{\infty} (I+R)\,\mathrm{d}X \approx 6.9 \text{ foxes km}^{-1},$$

giving $(KD/\beta)^{\frac{1}{2}} q_0 \approx 5.9$ foxes km^{-1}. For $p = \frac{1}{2}$ fox km^{-1}, (A2.8) gives an estimate of $t_c \approx 33$ for these values of the parameters, and so the ratio of the two exponentials e^{-dt_c} and $\mathrm{e}^{-\mu t_c}$ is approximately 3×10^{-6}, which justifies neglecting the smaller exponential in (A2.7) in the above analysis.

We now derive an estimate for the break width x_c. This involves solving the problem posed by (A2.1) and (A2.2). The first of (A2.1) gives

$$q(x, t) = 2q_0\delta(x)\,\mathrm{e}^{-\mu t}. \tag{A2.9}$$

Substituting this into the second equation gives

$$\partial r/\partial t = -dr + \partial^2 r/\partial x^2 + 2q_0\mu\delta(x)\,\mathrm{e}^{-\mu t}, \tag{A2.10}$$

the solution of which, with initial conditions (A2.2), is of the form

$$r(x, t) = (2r_0/\sqrt{\pi t})\exp(-x^2/4t - dt) + \mathrm{e}^{-\mu t} r^*(x, t),$$

where $r^*(x, t)$ is the solution of

$$\partial r^*/\partial t = (\mu - d)\,r^* + \partial^2 r^*/\partial x^2 + 2q_0\,\mu\delta(x) \tag{A2.11}$$

with homogeneous initial data. The last equation can be solved by using Laplace transforms. Denote the Laplace transform of r^*

$$\rho(x, s) = \int_0^{\infty} r^*(x, t)\,\mathrm{e}^{-st}\,\mathrm{d}t, \quad \mathrm{Re}\ s > 0.$$

Then ρ satisfies the inhomogeneous ordinary differential equation

$$\mathrm{d}^2\rho/\mathrm{d}x^2 + (\mu - d - s)\,\rho = -2q_0\mu\delta(x)/s, \quad -\infty < x < \infty, \quad \mathrm{Re}\ s > 0. \tag{A2.12}$$

Only the solution for $x \geqslant 0$ is of interest; it is given by

$$\rho(x, s) = \mu q_0\{\exp[-(s+d-\mu)^{\frac{1}{2}} x]\}/\{s(s+d-\mu)^{\frac{1}{2}}\}.$$

Thus, inverting the transform, we get

$$r^*(x, t) = (\mu q_0/2\pi\mathrm{i}) \int_C \{\exp[-(s+d-\mu)^{\frac{1}{2}} x]\}\,\mathrm{e}^{st}/\{s(s+d-\mu)^{\frac{1}{2}}\}\,\mathrm{d}s, \tag{A2.13}$$

where C is the Bromwich contour. The singularities of the integrand are a pole at $s = 0$ and a branch point at $s = -(d-\mu)$. The branch cut can be taken along the negative real axis to the left of the branch point, and so the contour of integration can be deformed to lie above and below the negative real axis. Since it is only necessary to evaluate $r^*(x, t)$ for $t = t_c$, it can be assumed that $t \gg 1$ in the integral (A2.13). Following Murray (1984, ch. 5), the main contribution to the integral is

then given by the residue at the pole $s = 0$; the contribution from the branch cut is exponentially small in comparison provided that

$$(x/2t)^2 \ll d-\mu. \tag{A2.14}$$

This inequality will be shown to hold below. Thus we arrive at the solution for $r(x, t)$ given by

$$r(x, t) \sim [2r_0/\sqrt{(\pi t)}] \exp [-x^2/4t - dt] + [\mu q_0/\sqrt{(d-\mu)}] \exp [-\mu t - (d-\mu)^{\frac{1}{2}} x]. \tag{A2.15}$$

To estimate the break width, note that the formula (A2.4) cannot be used directly since with (A2.9), $q(x, t)$ always involves a δ-function. Instead, we replace (A2.4) by

$$r(x_c, t_c) = mr(0, t_c) \tag{A2.4a}$$

The assumptions (A2.14) and $t \gg 1$ can again be used to justify neglecting the first term in (A2.15) with respect to the second. So from (A2.4a) and (A2.15), an estimate for the break width is given by

$$x_c \sim (d-\mu)^{\frac{1}{2}} \ln (1/m). \tag{A2.16}$$

If we take $m = 10^{-4}$ together with the parameters used previously to estimate t_c, then assumption (A2.14) is easily verified to be valid for $t = t_c$ and $x = x_c$ since $(x_c/2t_c)^2 \approx 0.05$ and $d-\mu = 0.38$.

Note that, at least to leading order, the formula for x_c is independent of the critical time t_c. The calculation of t_c was only necessary for the purpose of verifying the 't large' assumption that was made throughout the analysis in this appendix.

References

Anderson, R. M., Jackson, H. C., May, R. M. & Smith, A. M. 1981 Population dynamics of fox rabies in Europe. *Nature, Lond.* **289**, 765–771.

Andral, L., Artois, M., Aubert, M. F. A. & Blancou, J. 1982 Radiotracking of rabid foxes. *Comp. Immun. Microbiol. infect. Dis.* **5**, 285–291.

Artois, M. & Aubert, M. F. A. 1982 Structure des populations (age et sexe) de renard en zones indemnés ou atteintés de rage. *Comp. Immun. Microbiol. infect. Dis.* **5**, 237–245.

Bacon, P. J. (ed.) 1985 *Population dynamics of rabies in wildlife.* New York: Academic Press.

Baer, G. M. (ed.) 1975 *The natural history of rabies.* (Two volumes.) New York: Academic Press.

Boegel, K., Moegle, H., Steck, F., Krocza, W. & Andral, L. 1981 Assessment of fox control in areas of wildlife rabies. *Bull. Wld Hlth Org.* **59**, 269–279.

Gurtler, W. & Zimen, E. 1982 The use of baits to estimate fox numbers. *Comp. Immun. Microbiol. infect. Dis.* **5**, 277–283.

Jackson, H. C. & Schneider, L. G. 1984 Rabies in the Federal Republic of Germany, 1950–81: the influence of landscape. *Bull. Wld Hlth Org.* **62**, 99–106.

Källén, A., Arcuri, P. & Murray, J. D. 1985 A simple model for the spatial spread and control of rabies. *J. theor. Biol.* **116**, 377–393.

Lignieres, R. 1982 Prophylaxie de la Rage en France. *Comp. Immun. Microbiol. infect. Dis.* **5**, 377–382.

Lloyd, H. G., Jensen, B., Van Haaften, J. L., Niewold, F. J. J., Wandeler, A., Bogel, K. & Arata, A. A. 1976 Annual turnover of fox populations in Europe. *Zbl. Vet. Med.* **23**, 580–589.

Macdonald, D. W. 1980 *Rabies and wildlife: a biologist's perspective.* Oxford: Oxford University Press.

Macdonald, D. W., Bunce, R. G. H. & Bacon, P. J. 1981 Fox populations, habitat characterization and rabies control. *J. biogeogr.* **8**, 145–151.

Murray, J. D. 1984 *Asymptotic analysis*, 2nd edn. Heidelberg: Springer-Verlag.

Sikes, R. K. 1970 Rabies. In *Infectious diseases of wild mammals* (ed. D. O. Trainer), pp. 3–19. Ames, Iowa: Iowa State University Press.

Steck, F. & Wandeler, A. 1980 The epidemiology of fox rabies in Europe. *Epidem. Rev.* **2**, 71–96.

Toma, B. & Andral, L. 1977 Epidemiology of fox rabies. *Adv. Vir. Res.* **21**, 15.

Winkler, W. G. 1975 Fox rabies. In *The natural history of rabies*, vol. 2 (ed. G. M. Baer), pp. 3–22. New York: Academic Press.